

AD-A100 818 AIR FORCE INST OF TECH WRIGHT-PATTERSON AFB OH SCHOO--ETC F/G 11/6  
CRYSTALLIZATION KINETICS OF TWO METALLIC GLASSES BY MOSSBAUER S--ETC(II)  
MAR 81 D E BELLER  
UNCLASSIFIED AFIT/ANE/PH/81M-1

NL

1 OF 1  
AFIT/ANE/PH/81M-1

END  
DATE  
FILED  
7-81  
DTIC

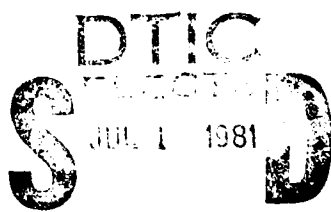
AD A 160 818

Accession For	
NTIS GRA&I	<input checked="" type="checkbox"/>
DTIC TAB	<input type="checkbox"/>
Unannounced	<input type="checkbox"/>
Justification	
By	
Distribution/	
Availability Codes	
Aveff and/or	
Dist	Special
A	

CRYSTALLIZATION KINETICS OF TWO  
METALLIC GLASSES BY MOSSBAUER  
SPECTROSCOPY.

Thesis,

Denis E. Beller  
AFIT/GNE/PH/81M-1 Captain USAF



Approved for public release; distribution unlimited.

AFIT/GNE/PH/81M-1

CRYSTALLIZATION KINETICS OF TWO METALLIC  
GLASSES BY MOSSBAUER SPECTROSCOPY

THESIS

Presented to the Faculty of the School of Engineering of  
of the Air Force Institute of Technology  
Air University  
In Partial Fulfillment of the  
Requirements for the Degree of  
Master of Science

by

Denis E. Beller, B.S.  
Captain USAF

Graduate Nuclear Engineering

March 1981

Approved for public release; distribution unlimited.

Preface

This thesis describes my efforts to determine the crystallization kinetics of two amorphous iron alloys,  $Fe_{80}B_{20}$  and  $Fe_{80}P_{6.5}C_{3.5}B_{10}$ . The objectives of this study were: 1) to anneal the glasses at various temperatures, 2) to take Mossbauer spectra during the annealing, 3) to analyze the spectra to determine the growth of crystals, and 4) to use the crystallization rates to calculate the activation energy and projected lifetimes at 473 K. This thesis will summarize past work in this area, describe the equipment and methods, and present analysis of the Mossbauer spectra and the results, conclusions and recommendations.

I thank Dr. Harold Gegel of the Air Force Materials Laboratory for sponsoring this study and supplying the glassy metal ribbons. I especially thank my advisor, Dr. George John, for his continuous support and guidance. Finally, I am grateful to my wife, Judy, and my sons, David and Timothy, for their constant devotion and support during this long study.

## Contents

	<u>Page</u>
Preface . . . . .	ii
List of Figures . . . . .	v
List of Tables . . . . .	vii
Abstract . . . . .	viii
I. Introduction . . . . .	1
Background . . . . .	1
Problem . . . . .	2
Scope . . . . .	2
Review of the Literature . . . . .	2
Assumptions . . . . .	5
Overview . . . . .	5
II. Theory . . . . .	6
III. Equipment and Procedures . . . . .	10
Mossbauer Equipment . . . . .	10
Annealing System . . . . .	10
Sample Preparation . . . . .	13
Heater Assembly . . . . .	13
Annealing and Data Collection . . . . .	14
Data Processing . . . . .	15
Subroutine CALFUN (Gaussian fit to Fe <sub>80</sub> B <sub>20</sub> glass) . . . . .	15
Subroutine CALFUN (Crystallized Fe <sub>80</sub> B <sub>20</sub> ) . . . . .	16
Subroutine CALFUN (for α-Fe, peaks one and six) . . . . .	17
Goodness of Fit . . . . .	18
IV. Results and Discussion . . . . .	19
Discussion . . . . .	36
V. Conclusions and Recommendations . . . . .	40
Recommendations . . . . .	40

	<u>Page</u>
Bibliography . . . . .	42
APPENDIX A: GAUSSCALF . . . . .	44
APPENDIX B: FIVECALF . . . . .	48
APPENDIX C: ALPHA-BG . . . . .	54
APPENDIX D: GENFIT Instructions . . . . .	58
APPENDIX E: Applications of Metallic Glasses . . . . .	62
Vita . . . . .	65

List of Figures

<u>Figure</u>	<u>Page</u>
1 Heater . . . . .	11
2 Mossbauer/Annealing System . . . . .	12
3 Sample/Heater Assembly . . . . .	14
4 Mossbauer Spectrum of $\text{Fe}_{80}\text{B}_{20}$ , 573 K, 2.08 Hr, GAUSSCALF, $x = 0$ . . . . .	21
5 Mossbauer Spectrum of $\text{Fe}_{80}\text{B}_{20}$ , 573 K, 48.9 Hr, GAUSSCALF, $x = 0$ . . . . .	22
6 Mossbauer Spectrum of $\text{Fe}_{80}\text{B}_{20}$ , 573 K, 111 Hr, FIVECALF, $x = 0.0512$ . . . . .	23
7 Mossbauer Spectrum of $\text{Fe}_{80}\text{B}_{20}$ , 573 K, 281 Hr, FIVECALF, $x = 0.190$ . . . . .	24
8 Mossbauer Spectrum of $\text{Fe}_{80}\text{B}_{20}$ , 573 K, Fully Crystallized, FIVECALF. . . . .	25
9 Mossbauer Spectrum of $\text{Fe}_{80}\text{B}_{20}$ , 611 K, Fully Crystallized, FIVECALF. . . . .	26
10 Mossbauer Spectrum of $\text{Fe}_{80}\text{B}_{20}$ , 611 K, Fully Crystallized, FIVECALF with Quadrupole Splitting. . . . .	27
11 Mossbauer Spectrum of $\text{Fe}_{80}\text{B}_{20}$ , 611 K, Run 3 Fully Crystallized, FIVECALF. . . . .	28
12 Mossbauer Spectrum of $\text{Fe}_{80}\text{B}_{20}$ , 604 K, 13.8 Hr, FIVECALF, $x = 0.316$ . . . . .	29
13 Mossbauer Spectrum of $\text{Fe}_{80}\text{B}_{20}$ , 604 K, Fully Crystallized, FIVECALF. . . . .	30

<u>Figure</u>	<u>Page</u>
14 Mossbauer Spectrum of $Fe_{80}P_{6.5}C_{3.5}B_{10}$ , 716 K, 2.87 Hr, ALPHA-BG, $x \approx 1$ . . . . .	31
15 Mossbauer Spectrum of $Fe_{80}P_{6.5}C_{3.5}B_{10}$ , 716 K, Fully Crystallized, ALPHA-BG . . . . .	32
16 Crystallized Fraction $x(t)$ vs Time. . . . .	34
17 Arrhenius Plot. . . . .	35

List of Tables

<u>Table</u>	<u>Page</u>
I Annealing Runs . . . . .	20

Abstract

In this study, Mossbauer spectroscopy was used to examine thermal aging of two metallic glasses.  $Fe_{80}B_{20}$  was isothermally annealed at 573, 604, 611, and 626 K; and  $Fe_{80}P_{6.5}C_{3.5}B_{10}$  was annealed at 614, 716, and 744 K. The activation energy of  $Fe_{80}B_{20}$ , determined from the growth of  $\alpha$ -Fe crystals, was  $0.256 \pm 0.006$  MJ/mole. The projected lifetime of this glass, based on the onset of crystallization, is 400 years. No quantitative data were obtained for  $Fe_{80}P_{6.5}C_{3.5}B_{10}$ ; however, based on the higher temperature required for crystallization, it is expected to have a longer lifetime.

CRYSTALLIZATION KINETICS OF TWO METALLIC  
GLASSES BY MOSSBAUER SPECTROSCOPY

I. Introduction

Mossbauer spectroscopy is becoming an increasingly important tool for studying the environments of nuclei. In this study, it was used to examine the crystallization characteristics of  $Fe_{80}B_{20}$  and  $Fe_{80}P_{6.5}C_{3.5}B_{10}$  amorphous alloys. These materials, commonly called metallic glasses, crystallize during accelerated aging at high temperatures.

Background

The glassy metals exhibit useful magnetic, as well as material (tensile strength, hardness, flexibility), properties.<sup>1</sup> The Air Force Materials Laboratory has become interested in their possible use in magnetic devices for Air Force weapons systems. As a result of this interest, in 1978 Schmidt (Ref 1) and Roberts (Ref 2) used Mossbauer spectroscopy to study the atomic structure of a few of the glassy metals, including  $Fe_{80}B_{20}$ . Because of projected high-temperature applications, the Materials Laboratory is concerned about thermal aging of these materials. Knowledge of the glasses' expected lifetimes at operating temperatures around 473 K is needed. To predict the aging rates of these amorphous materials, one must know

---

<sup>1</sup>See Appendix E for a review of possible applications.

their crystallization characteristics. Many methods have been used to determine these rates; all require measurements at 100 to 200 K above the expected operating temperature. In this study, Mossbauer spectroscopy was used to examine the growth of crystals in the metallic glasses  $Fe_{80}B_{20}$  and  $Fe_{80}P_{6.5}C_{3.5}B_{10}$ .

#### Problem

The problem investigated in this study was to determine the thermal aging rate of metallic glasses. Specifically, the kinetics of crystallization of  $Fe_{80}B_{20}$  and  $Fe_{80}P_{6.5}C_{3.5}B_{10}$  were studied. These glasses were examined by: 1) isothermal annealing, 2) taking Mossbauer spectroscopy during annealing, 3) evaluating the spectra to determine growth of  $\alpha$ -Fe crystals, and 4) using the crystallization rates at various temperatures to determine the Arrhenius constant.

#### Scope

This study was limited to the investigation of only two of the glassy metals,  $Fe_{80}B_{20}$  and  $Fe_{80}P_{6.5}C_{3.5}B_{10}$ . The temperature ranges were respectively 573 to 626 K and 716 to 744 K. The annealing periods were from one day at the high temperatures to two weeks at the lowest temperatures. No attempt was made to determine the structure of either the amorphous or the crystalline material. In addition, the literature studied was limited to only sources available at the School of Engineering, Air Force Institute of Technology.

#### Review of the Literature

This section contains a review of some of the many studies of the metallic glasses. These studies are mainly

concerned with three characteristics of the glasses: 1) amorphous structure, 2) temperature dependence of their magnetic properties, and 3) thermal aging (or crystallization) characteristics. Some of the results of these studies will be presented in the discussion section in Chapter IV.

Luborsky studied the crystallization of  $\text{Fe}_{80}\text{B}_{20}$ ,  $\text{Fe}_{40}\text{Ni}_{40}\text{P}_{14}\text{B}_6$ , and  $\text{Fe}_{40}\text{Ni}_{40}\text{B}_{20}$ , using magnetic methods and differential scanning calorimetry (Ref 3). Using the temperature of onset of crystallization at various heating rates, he determined the activation energy for the three materials. He also showed that thermal stability increased with the number of atomic species, i.e., that  $\text{Fe}_{80}\text{B}_{20}$  was the least stable of the three glasses. Fukamichi and others studied the magnetization, electrical resistivity, thermal expansion, and differential thermal change of a variety of Fe-B glasses (Ref 4). They determined that the crystallization mechanism of the Fe-B glasses depended on the concentration of boron. Chien studied  $\text{Fe}_{80}\text{B}_{20}$  from 4.2 K up to 1050 K, using Mossbauer spectroscopy, and found that it crystallized to  $\alpha$ -Fe and  $\text{Fe}_3\text{B}$  when annealed at a high heating rate, but found only  $\text{Fe}_2\text{B}$  at low heating rates (Ref 5). Luborsky and Lieberman examined the crystallization kinetics of the Fe-B glasses (12 to 28 percent boron) by differential scanning calorimetry (Ref 6). They determined that for 18 to 28 percent boron, the activation energy for the onset of crystallization was independent of boron concentration. However, Tarnoczi and others studied the role of  $\text{Fe}_3\text{B}$  in the crystallization of Fe-B glasses, and concluded

that  $\text{Fe}_{80}\text{B}_{20}$  was most stable (Ref 7). Matsuura, in a study similar to Luborsky and Lieberman's above, used differential thermal analysis on 12 to 20 percent boron Fe-B glasses (Ref 8). His results, obtained above 700 K, led to the conclusion that the formation of  $\alpha$ -Fe accompanies the crystallization of  $\text{Fe}_3\text{B}$ . Chien and others did a lengthy study on Fe-B glasses (14 to 28 percent boron) and crystalline  $\text{Fe}_3\text{B}$  using Mossbauer spectroscopy and magnetization measurements (Ref 9). Kemeny and others used Mossbauer spectroscopy, differential scanning calorimetry, and magnetization measurements for a thorough investigation of the structure and crystallization of Fe-B metallic glasses (12 to 25 percent boron) (Ref 10). For 16 to 25 percent boron, they concluded that crystallization proceeds by the formation of  $\alpha$ -Fe and  $\text{Fe}_3\text{B}$  in an eutectic process. They also deduced that the glass structure should be based on locally distorted, quasi-crystalline  $\text{Fe}_3\text{B}$ . Schaafsma and others have also done a lengthy crystallization study on two  $\text{Fe}_{80}\text{B}_{20}$  glasses (Ref 11). They concluded that the crystallization mechanism did not change between 580 and 640 K. They also found that nucleation did not control the crystallization rate; i.e., that crystal nuclei exist in the as-quenched amorphous material. Finally, Kopcewicz used Mossbauer spectroscopy to study radio-frequency annealing of  $\text{Fe}_{40}\text{Ni}_{40}\text{B}_{20}$  (Ref 12). He found that as a result of magnetostriictively induced atomic vibrations, a strong rf field caused crystallization in  $\text{LN}_2$ -cooled samples.

### Assumptions

The following were assumed to be true at the outset:

- 1) The  $\text{Fe}_{80}\text{B}_{20}$  and  $\text{Fe}_{80}\text{P}_{6.5}\text{C}_{3.5}\text{B}_{10}$  alloys were amorphous.
- 2) During annealing  $\alpha$ -Fe and metastable  $\text{Fe}_3\text{B}$  were formed.
- 3) The compositions were true to within one percent.

### Overview

The theory of the Mossbauer effect has been well documented and will not be presented here; however, the use of Mossbauer spectroscopy to study nuclear environments is presented in Chapter II, along with the theory of crystallization of Fe-B glasses. The Mossbauer equipment, annealing system, experimental procedures, and data processing are described in Chapter III. Chapter IV contains the results and discussion, and Chapter V contains the conclusions and recommendations.

## II. Theory

The theory of the Mossbauer effect has been fully developed and is well understood (see, e.g., Ref 13 and 14). For a condensed and simplified explanation, see Roberts' thesis (Ref 2: 3-11). Mossbauer spectroscopy measures the hyperfine fields of nuclei. This is possible because the hyperfine field interacts with the nuclear dipole moment, which, for iron-57, splits the resonant-absorption energy into six energy levels. The magnitudes of these energies are directly proportional to the value of the hyperfine field, which is characteristic of the electron environment of the nucleus. Thus, for nuclei in a crystal, there are different six-peak spectra (with Lorentzian line shapes) for each magnetically inequivalent site. For an amorphous material which has only short-range order, there are very few magnetically equivalent sites. The glass spectrum, then, is a combination of many different six-peak spectra, with a probability distribution  $P(H)$  describing the nuclear hyperfine fields. The  $P(H)$  of  $\text{Fe}_{80}\text{B}_{20}$  have been described by Schmidt (Ref 1) and Vincze (Ref 15) as a binomial distribution. This distribution was related to the number of nearest neighbors of iron and non-iron nuclei. However, others have shown that the glass spectra can be described by a model-independent probability distribution (Refs 15, 16, and 17). Schurer and

and Morrish have shown that a single six-line pattern, using Gaussian line shapes, describes the glass spectrum reasonably well (Ref 16: 819). This method is used in this study for the  $\text{Fe}_{80}\text{B}_{20}$  glass.

When a metastable metallic glass is heated, it undergoes atomic rearrangement to a more stable, but still amorphous, state (Ref 18: 577). With further heating, it begins to crystallize. This crystallization has been described as a diffusion process, as one or more species migrates out of the amorphous region (Ref 11: 4428). For the Fe-B glasses, the possible crystalline states are  $\alpha$ -Fe, FeB,  $\text{Fe}_2\text{B}$ , and  $\text{Fe}_3\text{B}$ .  $\text{Fe}_2\text{B}$  is expected to form during crystallization of the amorphous phase because it is much more stable than  $\text{Fe}_3\text{B}$ . For  $\text{Fe}_{80}\text{B}_{20}$ , however, the metastable  $\text{Fe}_3\text{B}$  (or  $\text{Fe}_{75}\text{B}_{25}$ ) is much nearer the original composition than  $\text{Fe}_2\text{P}$  (or  $\text{Fe}_{67}\text{B}_{33}$ ). Thus, others have found that  $\alpha$ -Fe and  $\text{Fe}_3\text{B}$  are the species formed during annealing of  $\text{Fe}_{80}\text{B}_{20}$  (Refs 7: 1026; 8:232; 10: 485; 11: 4429). While some determined that iron diffused from the glass to form  $\alpha$ -Fe, leaving amorphous  $\text{Fe}_{75}\text{B}_{25}$ , which subsequently crystallized to  $\text{Fe}_3\text{B}$  (Ref 11: 4429), others deduced that  $\text{Fe}_3\text{B}$  crystallized accompanied by the simultaneous formation of  $\alpha$ -Fe (Ref 8: 233). For a glass with many species, such as  $\text{Fe}_{80}\text{P}_{6.5}\text{C}_{3.5}\text{B}_{10}$ , there are many possible crystalline states. These include FeB,  $\text{Fe}_2\text{B}$ ,  $\text{Fe}_3\text{B}$ ,  $\text{Fe}_3\text{C}$ ,  $\text{Fe}_5\text{C}$ , and combinations of these by atomic substitution, also  $\alpha$ -Fe.

The isothermal crystallization of an iron-based glass can be followed, then, by examining the growth of the six-peak

$\alpha$ -Fe spectrum in a series of Mossbauer spectra. The crystalline fraction  $x(t)$  is the ratio of the volume of  $\alpha$ -Fe crystals formed at time  $t$  to the volume in the fully crystallized sample. It can be described by the Johnson-Mehl-Avrami equation (Ref 11: 4426):

$$x(t) = 1 - \exp [-(k(T)t)^n] \quad (1)$$

When rearranged, Eq (1) becomes

$$\ln \ln \frac{1}{1-x(t)} = n \ln k(T) + n \ln t \quad (2)$$

which yields a straight line plot with slope  $n$ . Above,  $k(T)$  is a temperature dependent constant, and the exponent  $n$  is determined by the nucleation and growth characteristics of the crystallization. The time  $t_x(T)$  to crystallized fraction  $x$  can be determined from Eq (2) for a series of isothermal measurements. Then, for a thermally-activated diffusion process, the Arrhenius equation describes the lifetime  $t_x$  at constant  $x$  as a function of temperature  $T$ :

$$t_x = k_0^{-1} \exp (E_A/k_B T) \quad (3)$$

where  $k_0$  is a frequency factor,  $k_B$  is the Boltzman constant, and  $E_A$  is the activation energy of the crystallization process expressed as energy per atom (or per mole) (Ref 11: 4427). Eq (3), when rearranged, also yields a straight line plot, with slope  $E_A/k_B$ :

$$\ln t_x = \ln k_0^{-1} + (E_A/k_B)T^{-1} \quad (4)$$

The above kinetic parameters can be derived from relatively quick measurements at high temperatures. If the assumption is valid that the crystallization process is the same over a large range of temperatures, then these constants can be used to predict the crystallization rate at lower temperatures. In this study, the crystallized fractions  $x(t)$  were determined from the amplitudes of the  $\alpha$ -Fe portions of Mossbauer spectra. The half lives  $t_{.5}$  were then determined by least-squares curve fitting, and were used to determine the activation energy from the Arrhenius plot.

### III. Equipment and Procedures

In this section the Mossbauer spectroscopy equipment and annealing system are described. The procedures for preparing the glass samples and assembling them in the heater are included. Annealing the samples, taking the Mossbauer spectra during annealing, and analyzing the spectra are also described.

#### Mossbauer Equipment

The major Mossbauer spectroscopy components included a constant-acceleration velocity transducer (motor), a linear amplifier/single channel analyzer, a krypton-filled proportional counter, and a Mossbauer control unit (MCU). All were manufactured by Ranger Electronics. The Mossbauer spectrum was taken on an RIDL 400 multichannel analyzer (MCA), operated in the time-sequential scaling mode. With the exception of the time-base oscillator, which was an RIDL model 54-6, the equipment is the same as that described by Skluzacek (Ref 19: 5-11), Schmidt (Ref 1: 11-15), and Roberts (Ref 2: 12). The source, connected directly to the motor, was approximately 6 mCi cobalt-57 in a rhodium foil.

#### Annealing System

The annealing system consisted of a heater, a thermocouple reader, a vacuum system, and one of two temperature controllers. Ranger Engineering built the heater (Fig 1) as

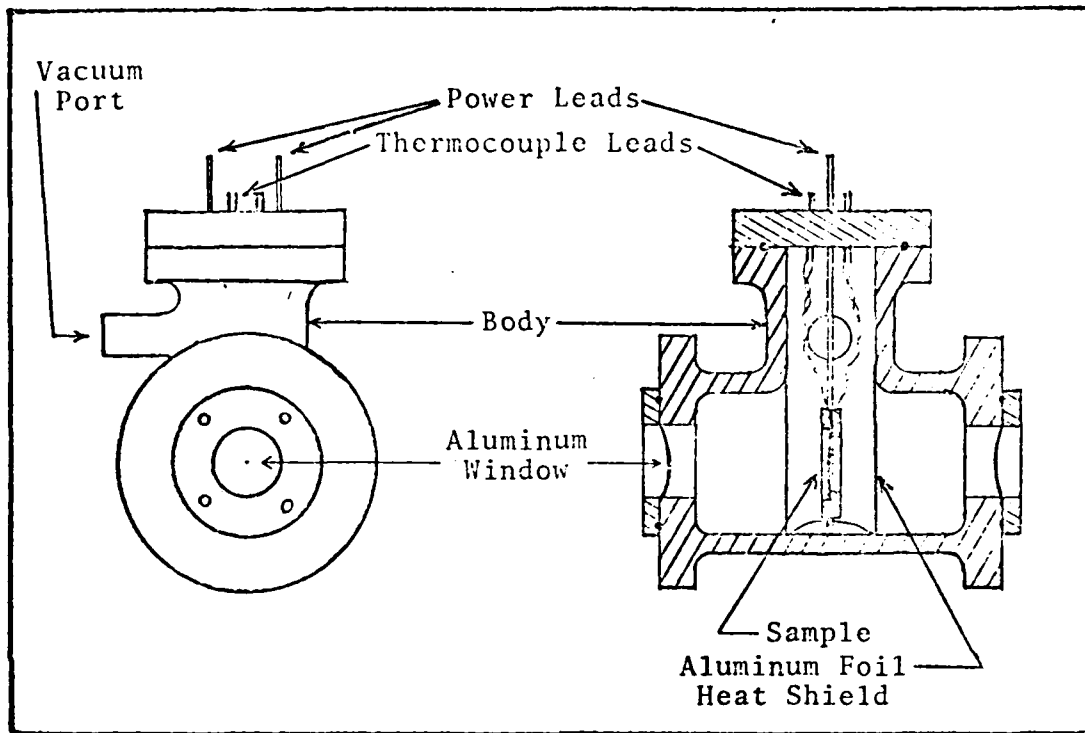


Fig 1. Heater (not to scale)

a prototype. The heating elements were two graphite discs ( $0.135 \pm 0.002$  mm x 25.4 mm). The sample was held between the heating discs and aligned with two aluminum foil windows ( $0.025 \pm 0.001$  mm x 25.4 mm). There were two iron-constantan thermocouples inside the heater; one was located in a slot at the edge of the heating element frame, the other was centered on the sample. The Omega thermocouple reader was calibrated with ice, boiling water, and molten tin. The vacuum system consisted of a forepump and an oil diffusion pump trapped with liquid nitrogen. Its purpose was to prevent convective heat transfer to the heater body. The first temperature controller,

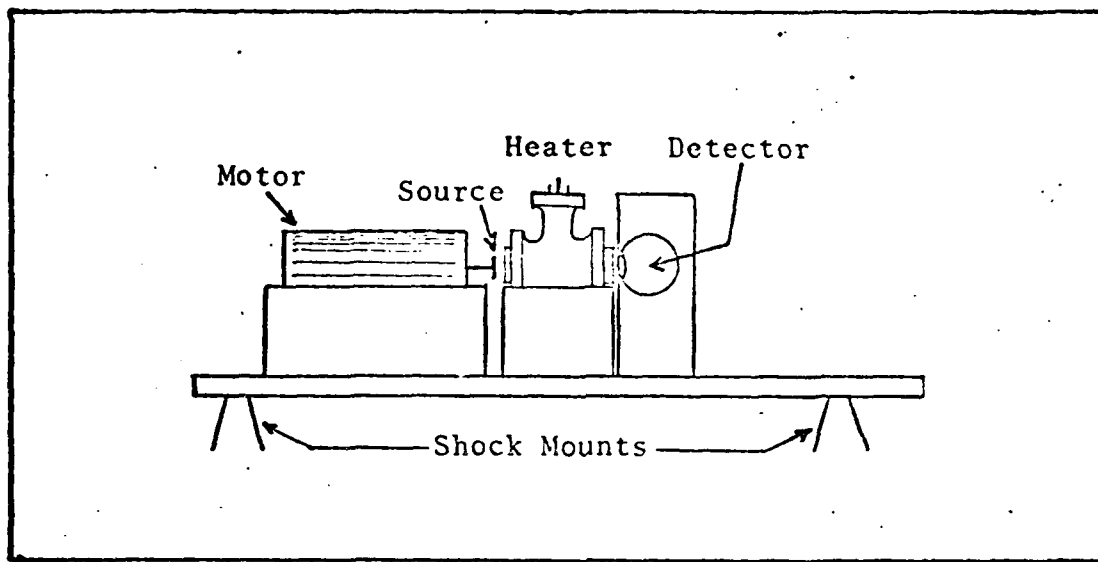


Fig 2. Mossbauer/A annealing System

a Lambda regulated DC power supply, was designed to provide manually-set constant current. Because of the failure of this power source, it was replaced with a Gardsman temperature controller, which was connected through a filament transformer to the heater. It supplied AC power, which produced an alternating field between the heating elements. This produced a problem which is discussed in Chapter IV. The edge thermocouple supplied feedback to the controller. Neither controller regulated the temperature adequately; temperatures varied  $\pm 2$  K throughout the runs, with occasional drops (less than 1% of annealing time) of up to 10 K.

A sketch of the source-absorber-detector is shown in Fig 2. The distance from the source to the detector window was approximately 10 cm.

### Sample Preparation

Dr. Harold Gegel, of the Air Force Materials Laboratory, provided the glassy metal ribbons which were used to prepare the samples. Battelle Laboratories at Columbus, Ohio, manufactured the ribbons by spin-cooling the molten alloy on a cooled rotating drum. The  $Fe_{80}B_{20}$  (nominal atom percent) glass ribbons were  $28.8 \pm 0.5 \mu m$  thick, the  $Fe_{80}P_{6.5}C_{3.5}B_{10}$  ribbons were  $27.9 \pm 0.5 \mu m$  thick, and the width of both varied from 0.5 to 1.2 mm with an average width of about 0.8 mm. The samples were prepared as a parallel array of the ribbons in  $32 \pm 2$  mm long strips, to form an absorber 25 mm wide. The strips were held parallel with cellophane tape at the top and bottom and then bonded at one end with cyanoacrylate cement to a boron nitride disc (25.4 mm diameter). This was done to prevent thermal stresses which have been observed to affect the spectra (Ref 20). When the cement had dried, the glass strips were trimmed to the dimension of the boron nitride disc. Since the cement degraded during the annealing, the strips were held unfettered and remained free of thermal stress.

### Heater Assembly

The sample and heating discs were assembled into the heater as shown in Fig 3. One graphite disc was inserted into the ceramic frame, followed by a clean boron nitride disc. The fine thermocouple was then centered on the boron nitride disc. The second boron nitride disc, with the glass sample attached, was then inserted, followed by the second graphite disc. The assembly was secured by two small plates and screws.

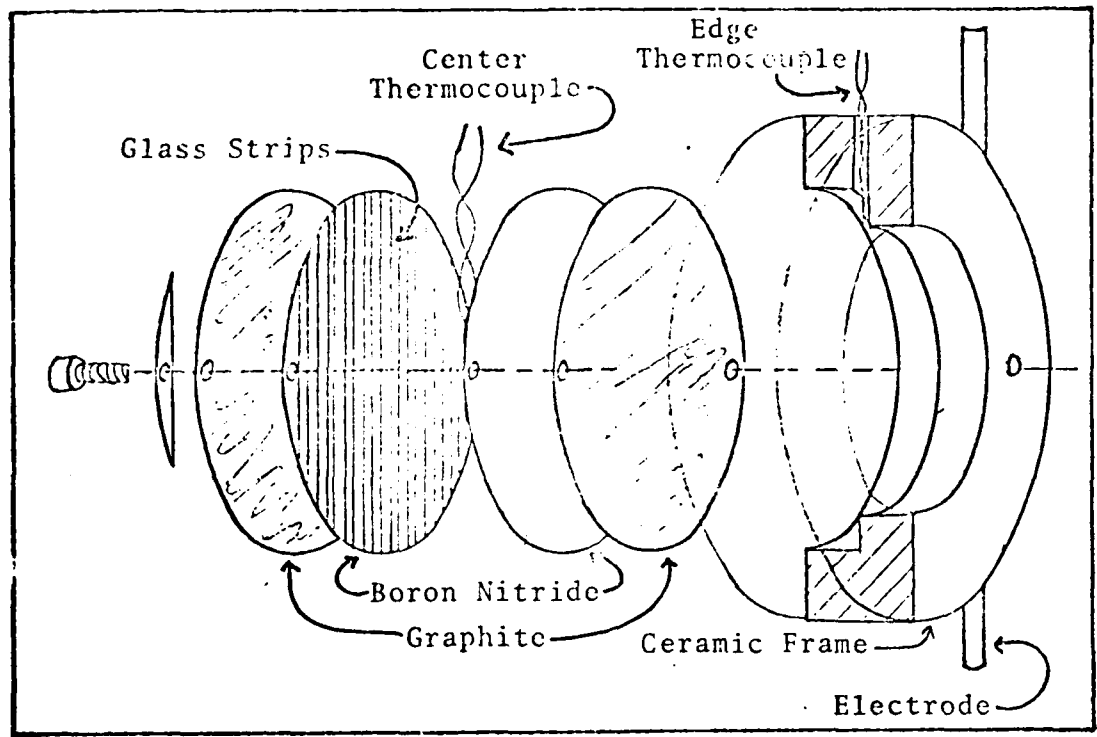


Fig 3. Sample/heater Assembly

The heater assembly was then inserted into the heater body, secured, and vacuum was applied.

#### Annealing and Data Collection

Once the heater was assembled and degassed overnight, the isothermal annealing run began. The heating rate was 5 to 15 K/min up to 473 K, and held there until again degassed. When the vacuum dropped below  $10^{-3}$  Pa, the temperature was increased to the desired annealing point. Generally, it took about five minutes. The initial Mossbauer spectrum was started as soon as this temperature was reached. Additional spectra were then taken in sequence until the sample was near full

crystallization. The time between the end of one spectrum and the beginning of the next was about ten minutes, which was the time necessary to punch the 400 channels of data onto paper tape. The isothermal annealing runs lasted from 10.5 hrs for  $\text{Fe}_{80}\text{B}_{20}$  at 626 K, up to 315 hrs for  $\text{Fe}_{80}\text{B}_{20}$  at 573 K. To fully crystallize the samples, the temperature was increased for about 18 hrs following each annealing run (to 640 K for  $\text{Fe}_{80}\text{B}_{20}$ , 750 K for  $\text{Fe}_{80}\text{P}_{6.5}\text{C}_{3.5}\text{B}_{10}$ ). The temperature was then lowered to the original annealing point, and a final Mossbauer spectrum was taken. The spectrum collection periods were between 1 and 24 hrs, depending upon the crystallization rate of the sample.

#### Data Processing

The Mossbauer spectra were analyzed by a least-squares minimization curve fitting program developed at the Argonne National Laboratory. This program, GENFIT, has been modified by Skluzacek (Ref 1: 21), Schmidt (Ref 1: 21-22), and Roberts (Ref 2: 18). It is listed as Appendix A of Roberts' thesis (Ref 2: 50-60), and will not be repeated here. A user-supplied subroutine, CALFUN, provides the mathematical model to be fitted, along with the desired variable parameters. Three different CALFUNS were used for this study. They are explained below.

Subroutine CALFUN (Gaussian fit to  $\text{Fe}_{80}\text{B}_{20}$  glass).  
This subroutine fits Gaussian line shapes to the  $\text{Fe}_{80}\text{B}_{20}$  glass spectra taken at the beginning of each annealing run, though

the method can lead to erroneous values of the average hyperfine field (Ref 10: 478), it did provide reasonable fits. Its purpose was to provide the glass spectra to be included in the CALFUN below. The variables which were included in this subroutine were:

1. Baseline: the average counts in the background of the Mossbauer spectrum.
2. Magnetic field: one value of average hyperfine field, in kOe (100 kOe = 7.96 MA/m).
3. Isomer shift: one value of average isomer shift for the glass, in mm/sec.
4. Quadrupole split: one value of average quadrupole split for the glass, in mm/sec.
5. Total intensity: one value for total intensity (average) of peaks one and six, expressed as a fraction.
6. Relative intensity: one value of the ratio of the average intensity of peaks two and five to the average intensity of peaks one and six.
7. Linewidths: six values of the full width at half maximum intensity (FWHM); one for each of the six Gaussian line shapes, in mm/sec.

The areal ratios of peaks three and four were constrained to one-third the area of peak one. This subroutine is listed as Appendix A. It was called GAUSSCALF.

Subroutine CALFUN (Crystallized Fe<sub>80</sub>R<sub>20</sub>). This subroutine provides for fitting the data with one six-peak  $\alpha$ -Fe

spectrum, three six-peak  $\text{Fe}_3\text{B}$  spectra, and one six-peak (Gaussian) glass spectrum. The variable parameters are:

1. Baseline: as in GAUSSCALF above.
2. Magnetic fields: one hyperfine field for  $\alpha$ -Fe and one each for three  $\text{Fe}_3\text{B}$  sites, in kOe.
3. Isomer shifts: one each for  $\alpha$ -Fe and the three  $\text{Fe}_3\text{P}$  sites, in mm/sec.
4. Linewidths: one value of FWHM for peaks one and six, one for peaks two and five, and one for peaks three and four, of all three  $\text{Fe}_3\text{B}$  sites, in mm/sec.
5. Total intensities: one value of total intensity for each of  $\alpha$ -Fe,  $\text{Fe}_3\text{B}$ , and the glass.

To simplify--and reduce the time and cost of--processing, this subroutine required many constraints. The glass spectrum was constrained to those parameters found in GAUSSCALF above, only its intensity was variable. The linewidth of  $\alpha$ -Fe was constrained to that value found for the fully crystallized spectrum, and all six peaks used this same value. The areal ratios were 3:2:1:1:2:3 for peaks 1:2:3:4:5:6 of  $\alpha$ -Fe and  $\text{Fe}_3\text{B}$ . The relative intensities of the three  $\text{Fe}_3\text{B}$  sites were 1:1:1, and their linewidths were constrained to be equal for similar peaks. Finally, the quadrupole splits of  $\alpha$ -Fe and the three  $\text{Fe}_3\text{B}$  sites were constrained to zero. This subroutine, called INVICALF, is listed as Appendix B.

Subroutine CALFUN (for  $\alpha$ -Fe, peaks one through six). This version of CALFUN provides for analysis of only peaks one and six of the  $\alpha$ -Fe crystallized from the glass. It includes a

Gaussian shaped background, and does not fit the center portion of the spectrum. The required variables are:

1. Baseline: as in GAUSSCALF.
2. Magnetic fields: one value for the  $\alpha$ -Fe hyperfine field, and one value for the background, in kOe.
3. Total intensities: one value for the total intensity of peaks one and six of  $\alpha$ -Fe, and one value for the background.
4. Linewidths: one value of FWHM for  $\alpha$ -Fe, and one value for the background, in mm/sec.
5. Isomer shifts: one value of isomer shift for  $\alpha$ -Fe and one value for the background, in mm/sec.

This subroutine is listed in Appendix C, and was called ALPHA-BG. Appendix D contains instructions for using GENFIT and CALFUN, and discusses required alterations to FIVECALF for spectra taken at other temperatures.

#### Goodness of Fit

The goodness of fit to the Mossbauer spectra is measured by Chi-squared, which is generated by GENFIT. Its value is defined by:

$$\text{Chi}^2 = \sum_{i=1}^N \frac{(\text{data point}_i - \text{calculated point}_i)^2}{\text{data point}_i} \quad (5)$$

where N is the number of data points fitted. Theoretically, the values of Chi-squared obtained for a number of spectra should be randomly distributed around the number of data points, in the limit approaching this number.

#### IV. Results and Discussion

In this section, the results of the spectra analyses and crystallization rate determinations are presented. These results are compared in the discussion to those derived by others. Table I lists the isothermal annealing runs with the sample material, temperature, annealing period, slope of the Johnson-Mehl-Avrami plot, crystallization half-life  $t_{.5}$ , and heater power (AC or DC). Figures 4 through 15 are examples of the Mossbauer spectra taken during the annealing runs. The title of each figure lists the sample material, temperature, annealed time, CALFUN used, and crystalline fraction. The crystalline fraction was calculated as the ratio of the value of the  $\alpha$ -Fe intensity of that run to the value of the fully crystallized state. Figures 4 (2.89 hr at 573 K) and 5 (48.9 hr at 573 K) show that the glass spectrum changes very little before crystallization. Figure 6 shows the  $\alpha$ -Fe peaks just after the onset of crystallization; note that the remainder of the spectrum still resembles the glass spectra. Figures 7 and 8 (19 and 100 percent crystallized) include the locations of the peaks of the  $\alpha$ -Fe and three  $Fe_3B$  spectra, along with the values of their hyperfine fields (in MA/m). Note that the values of the three  $Fe_3B$  fields increased with time, which was true of all isothermal annealing runs. However, the linewidths of these peaks decreased with time, as much as 50 percent. Figures 9 and 10

TABLE I  
Annealing Runs

Run	Glass	Temperature (K ± 2 K)	Annealing Period (hr)	Half-life (hr)	Slope n	Power Type
1	Fe <sub>80</sub> B <sub>20</sub>	573	315	604 ± 57	1.60±0.22	DC
2	Fe <sub>80</sub> B <sub>20</sub>	604	45	34.0 ± .5	1.77±.24	AC
3	Fe <sub>80</sub> B <sub>20</sub>	611	76	18.0 ± 0.7	1.50±0.06	DC
4	Fe <sub>80</sub> B <sub>20</sub>	611*	48	21.1 ± 1.8	1.17±0.08	DC
5	Fe <sub>80</sub> B <sub>20</sub>	626	10.5	6.69 ± 0.54	1.57±0.14	DC
6	Fe <sub>80</sub> P <sub>6.5</sub> C <sub>3.5</sub> B <sub>10</sub>	614	27	No crystallization observed	AC	
7	Fe <sub>80</sub> P <sub>6.5</sub> C <sub>3.5</sub> B <sub>10</sub>	716	48	<2.9	AC	
8	Fe <sub>80</sub> P <sub>6.5</sub> C <sub>3.5</sub> B <sub>10</sub>	744	25	<0.5	AC	

\*This sample was annealed 13 days at 573 K, and was about 22% crystallized at the beginning of this run.

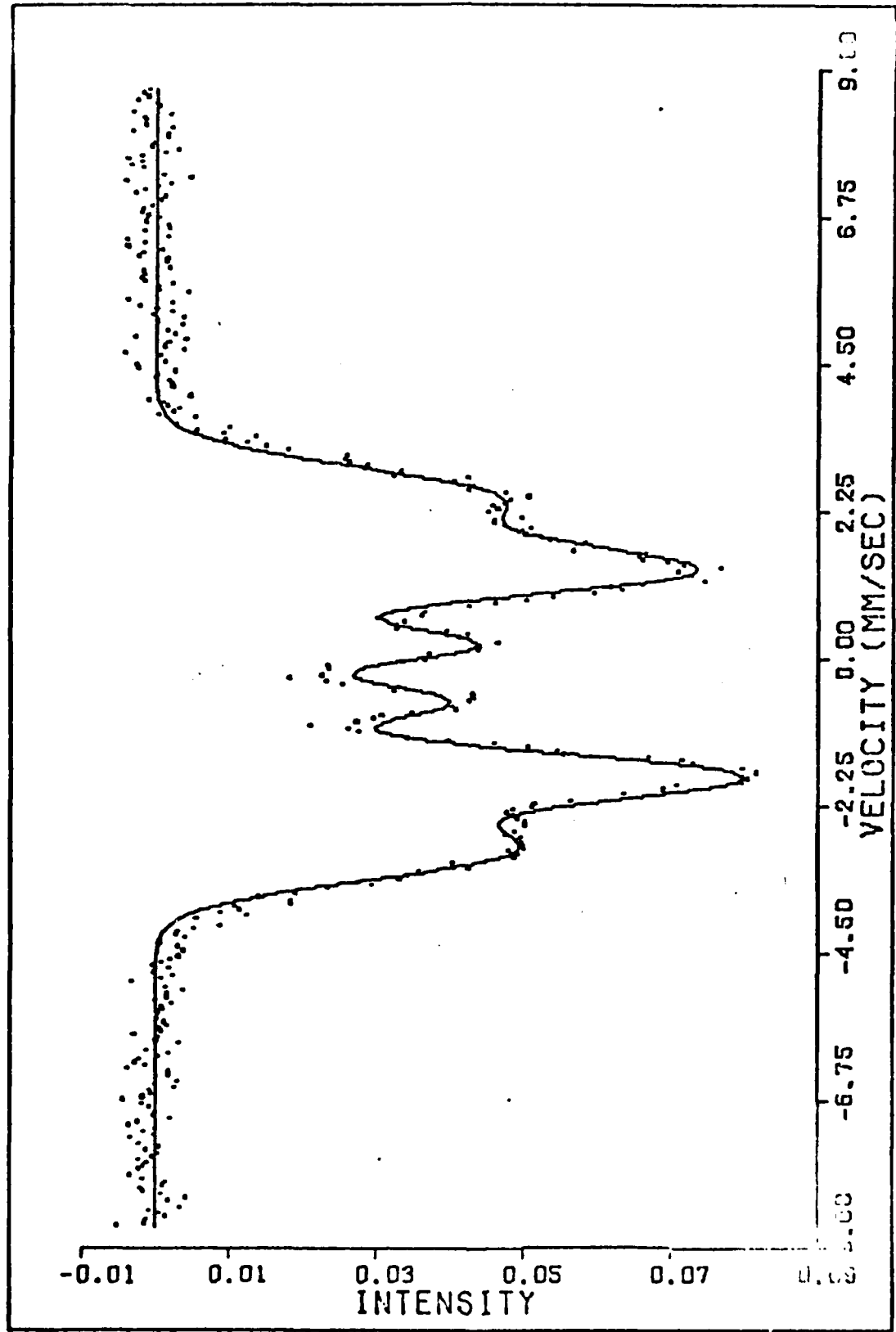


Fig. 4. Mossbauer Spectrum of  $\text{Fe}_{30}\text{B}_{20}$ , 573 K, 2.08 Hr, GAUSSCALF,  $x = 0$

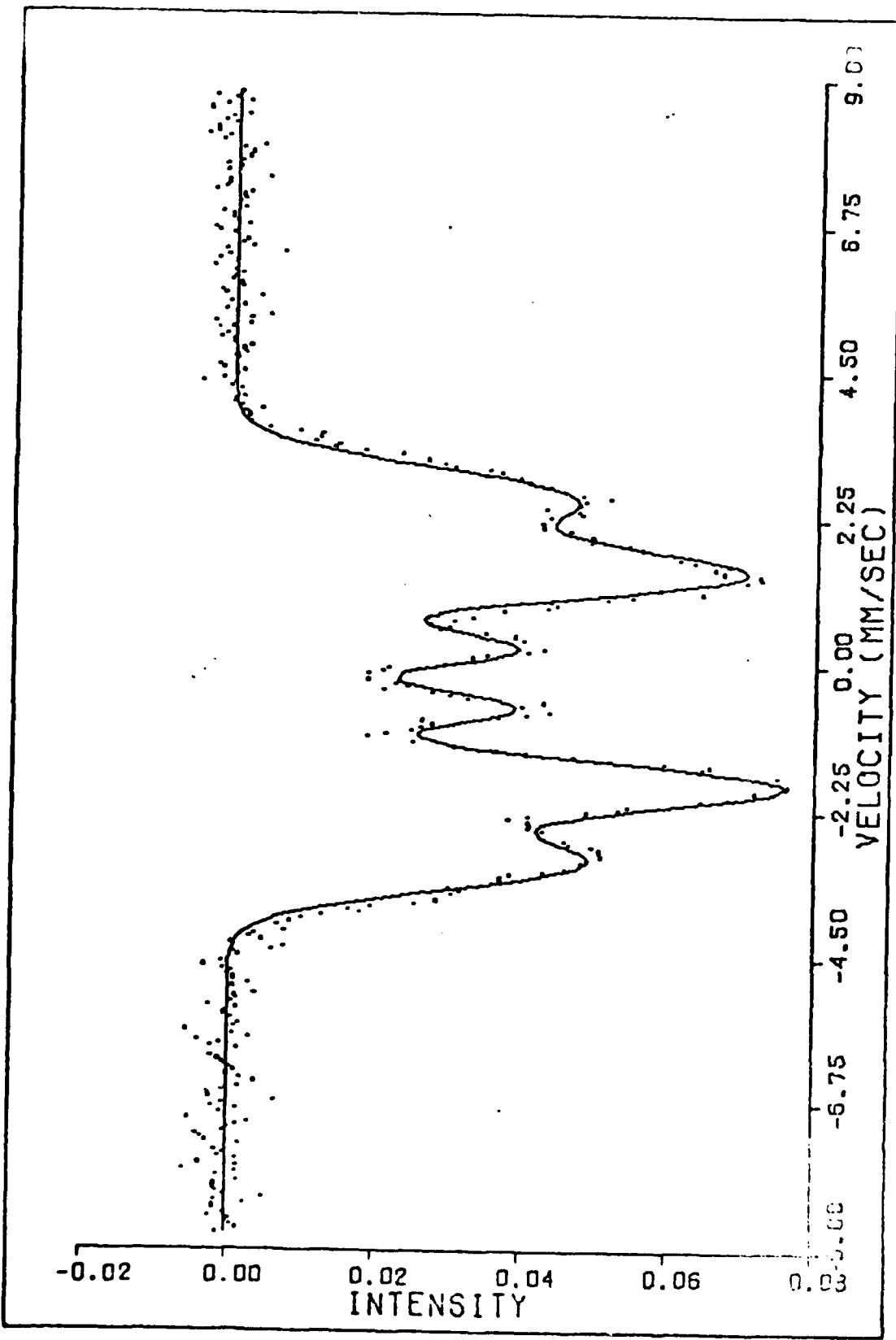


Fig. 5. Mossbauer Spectrum of  $\text{Fe}_{80}\text{B}_{20}$ , 573 K, 48.9 Hr, GAUSSCALF,  $x = 0$

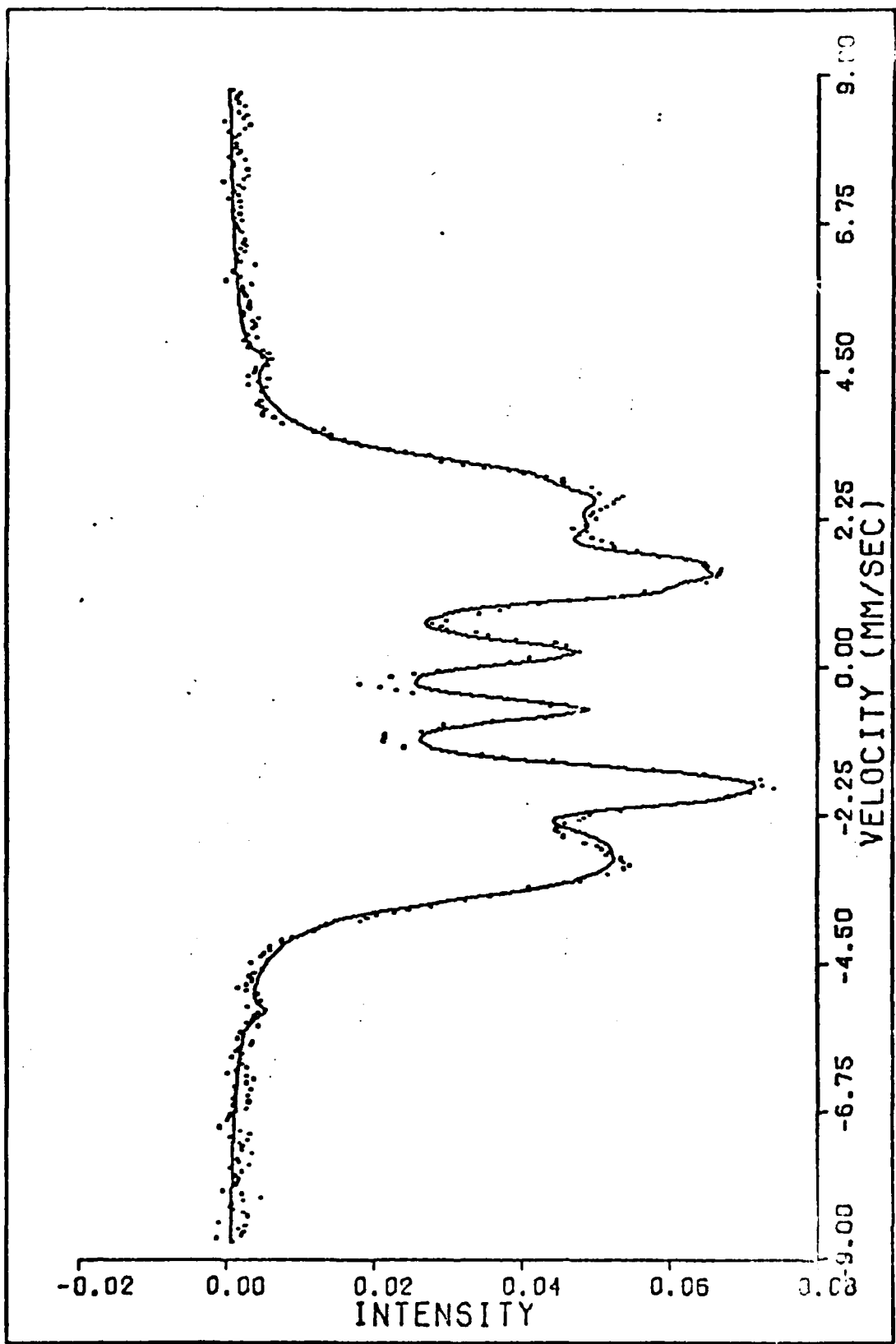


Fig. 6. Mossbauer Spectrum of  $\text{Fe}_{80}\text{B}_{20}$ , 573 K, 111 hr, FIVECALF,  $x = 0.0512$

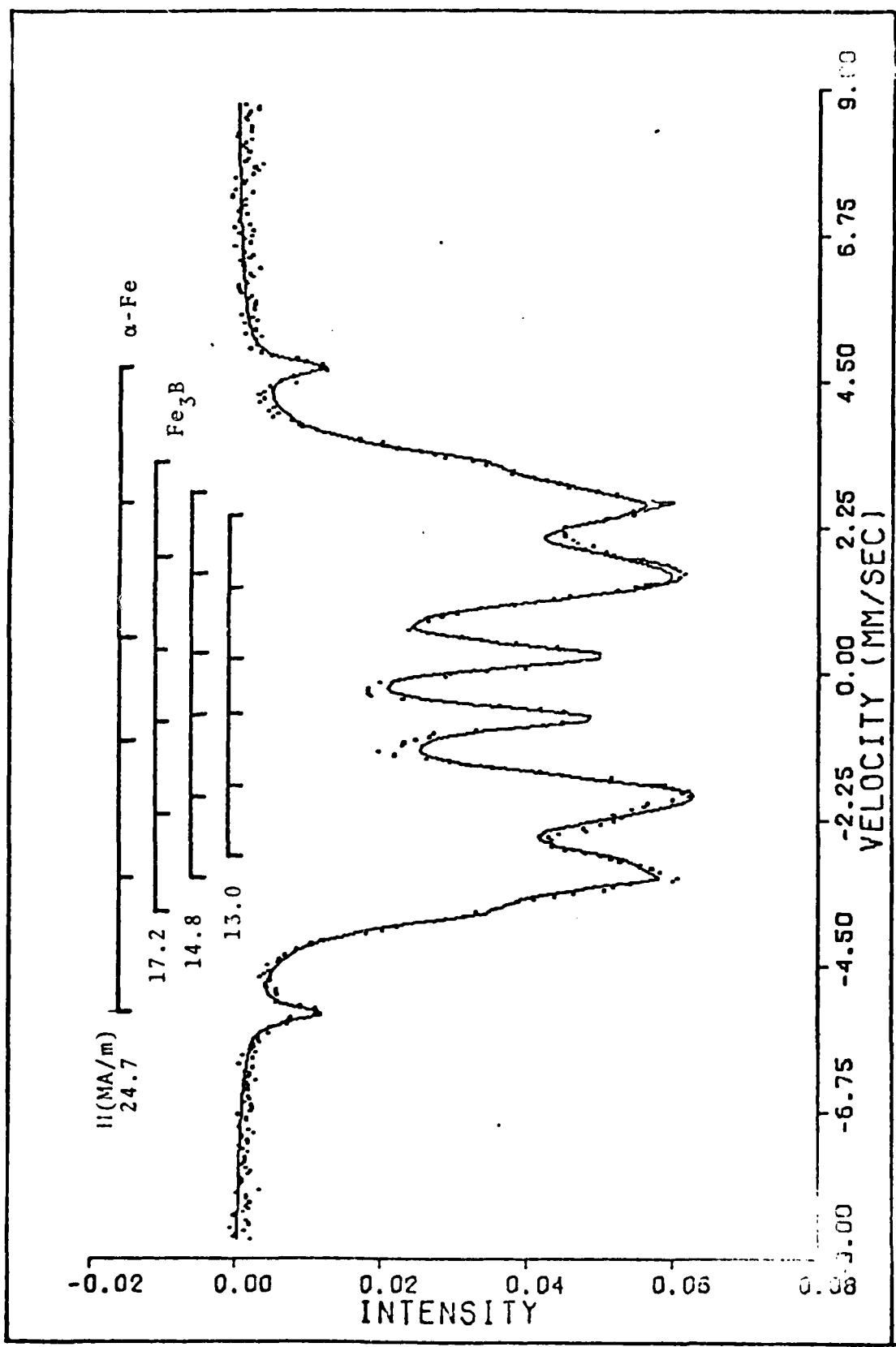
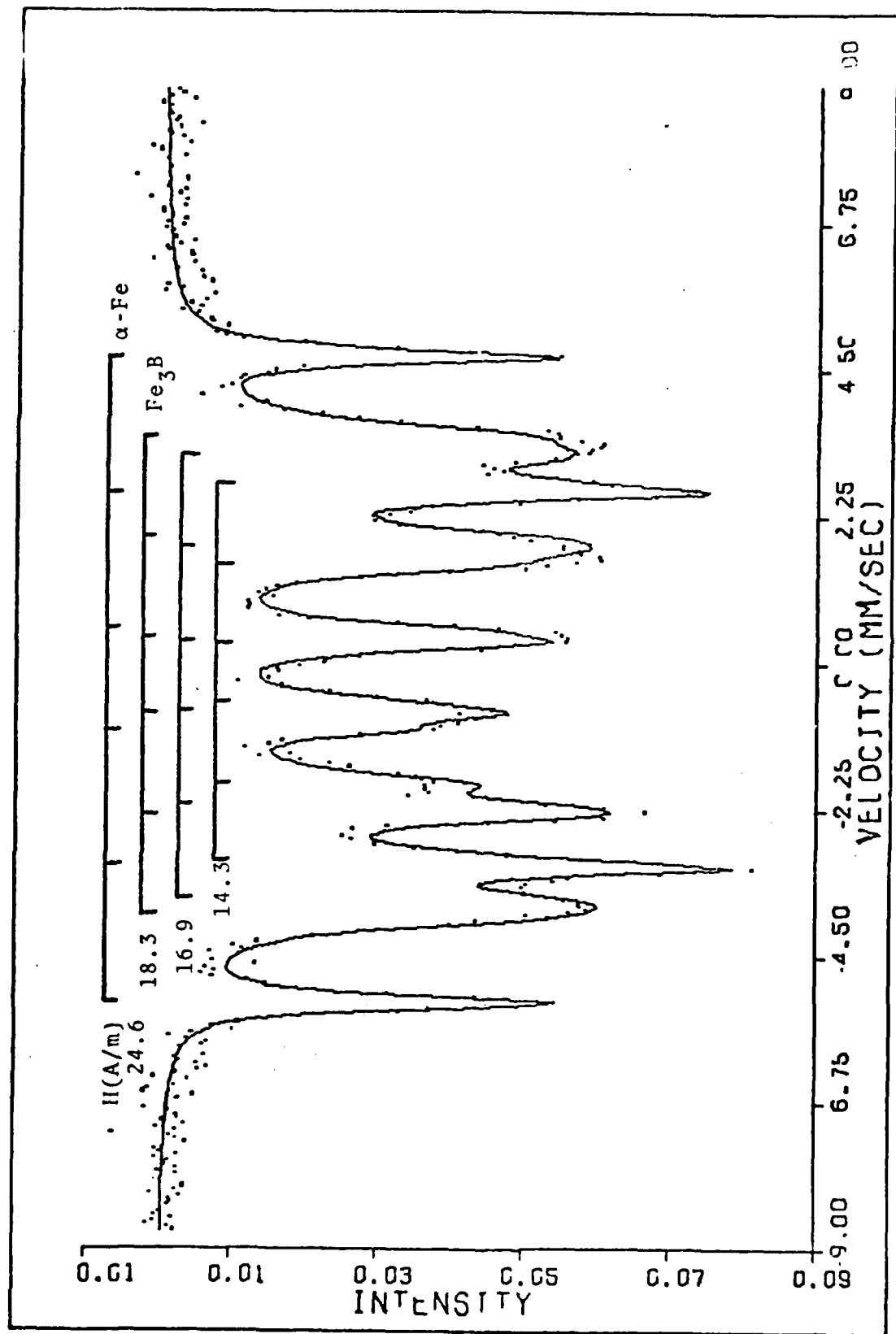


Fig. 7. Mossbauer Spectrum of  $\text{Fe}_{80}\text{B}_{20}$ , 573 K, 281 Hr, FIVECALF,  $x = 0.190$



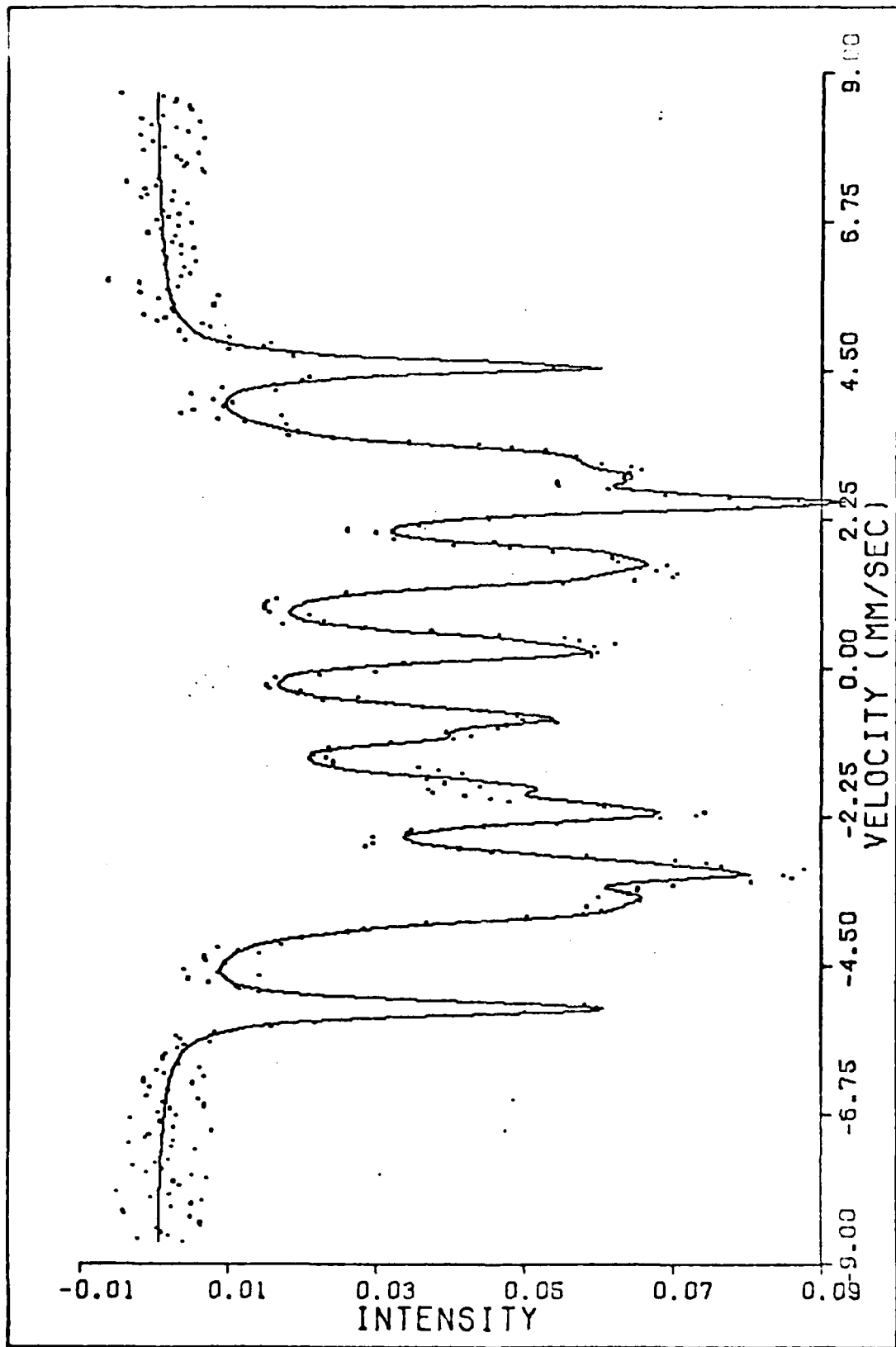


Fig. 9. Mossbauer Spectrum of  $\text{Fe}_{80}\text{B}_{20}$ , 611 K, Fully Crystallized, FIVECALF

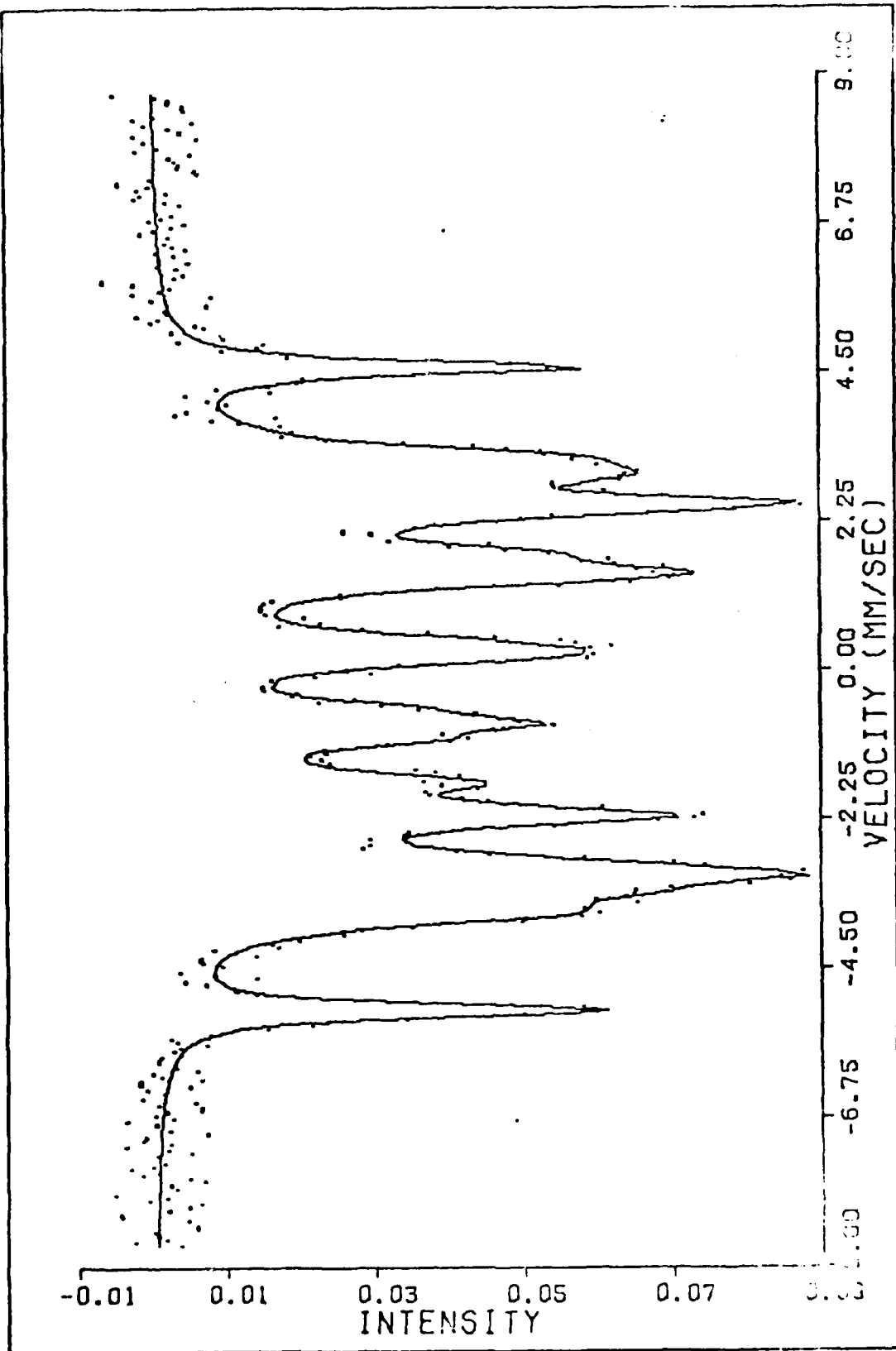


Fig 10. Mossbauer Spectrum of  $\text{Fe}_{30}\text{Rh}_{20}$ , 611 K, Fully Crystallized  
FIVECALF with Quadrupole Splitting

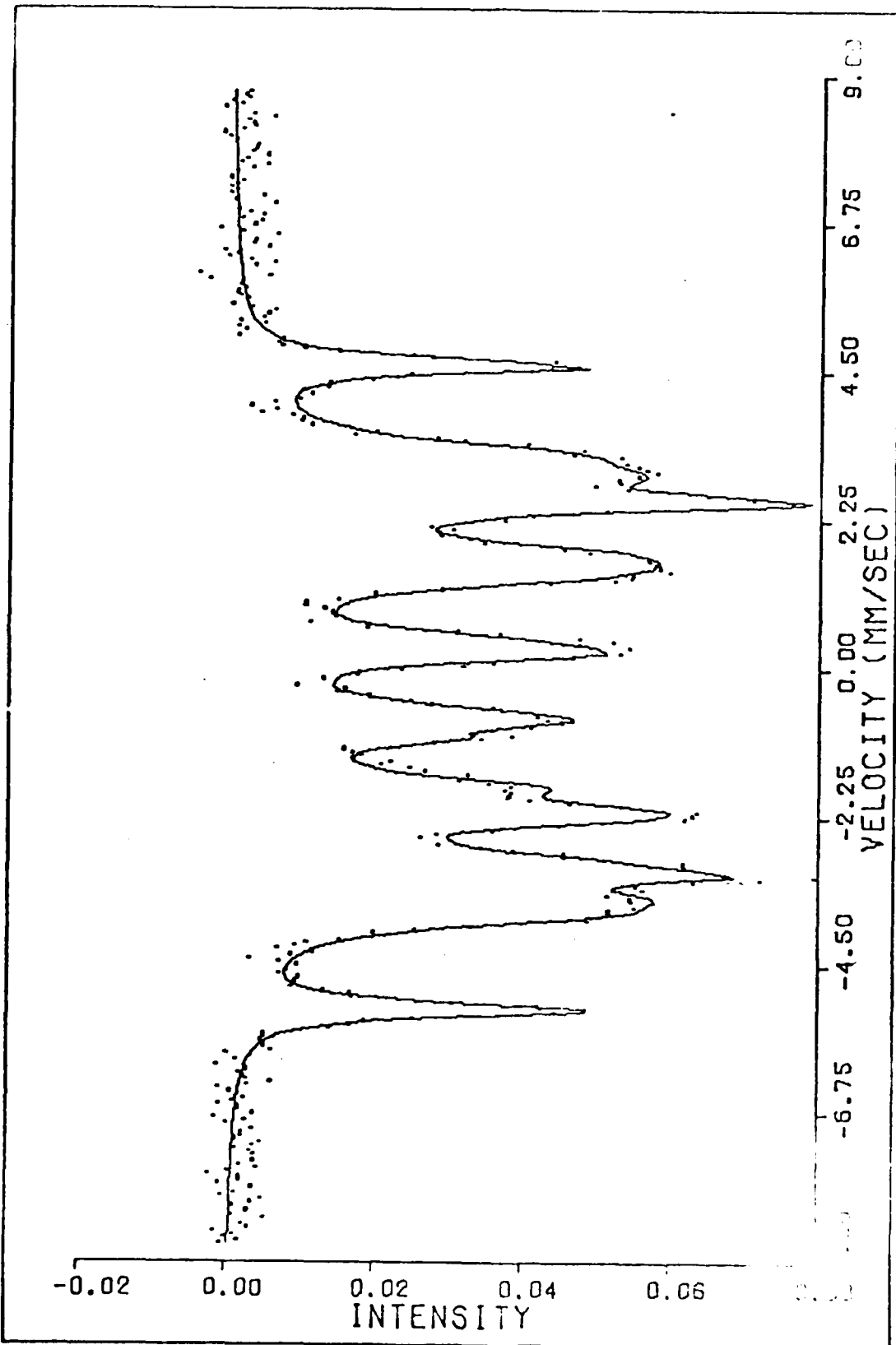


Fig. 11. Mossbauer Spectrum of  $\text{Fe}_{80}\text{B}_{20}$ , 611 K, Run 3, Fully Crystallized  
FIVECALF

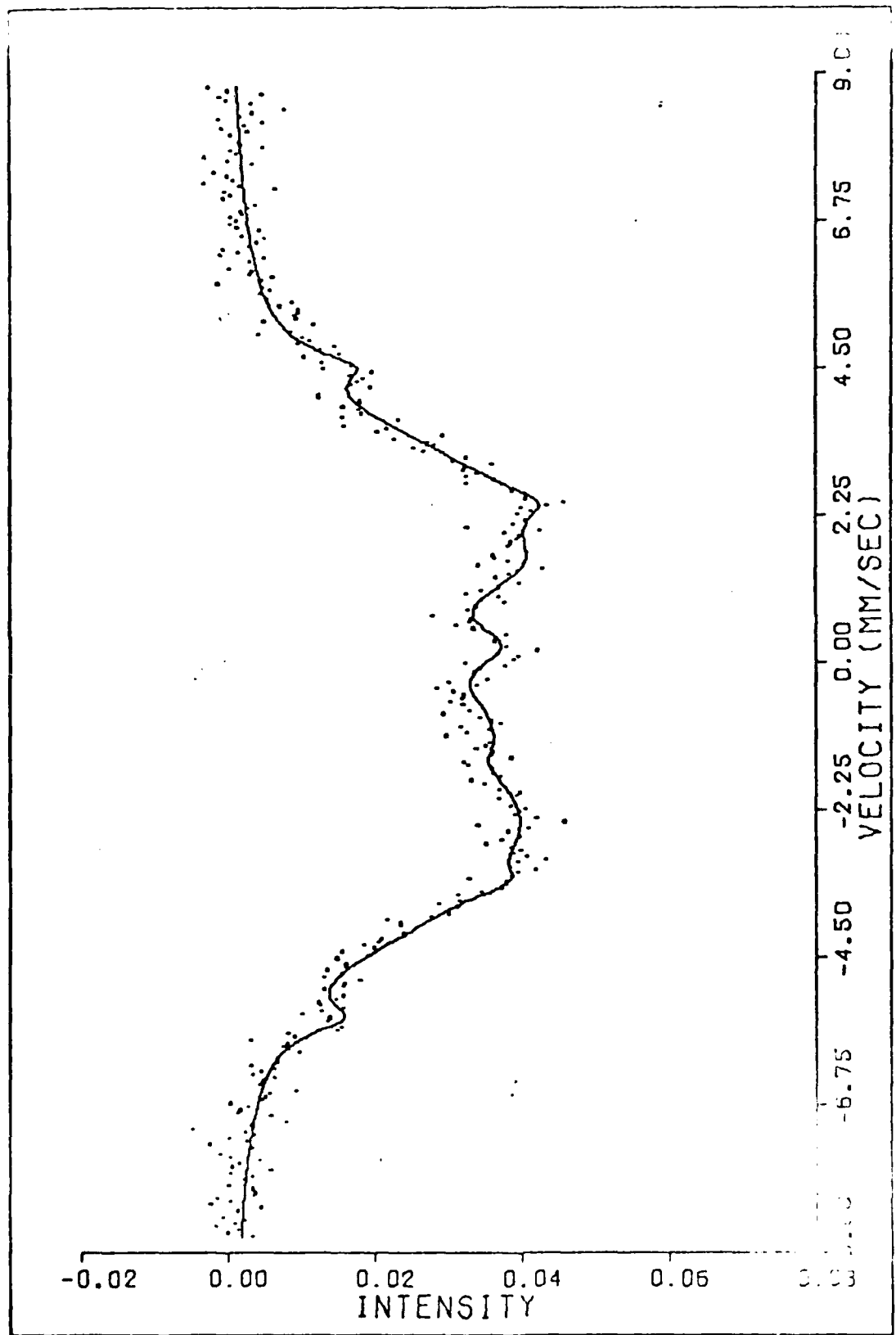


Fig. 12. Mossbauer Spectrum of  $\text{Fe}_{80}\text{B}_{20}$ , 604 K, 13.8 Hr, FIVECALF,  $\chi = 0.316$

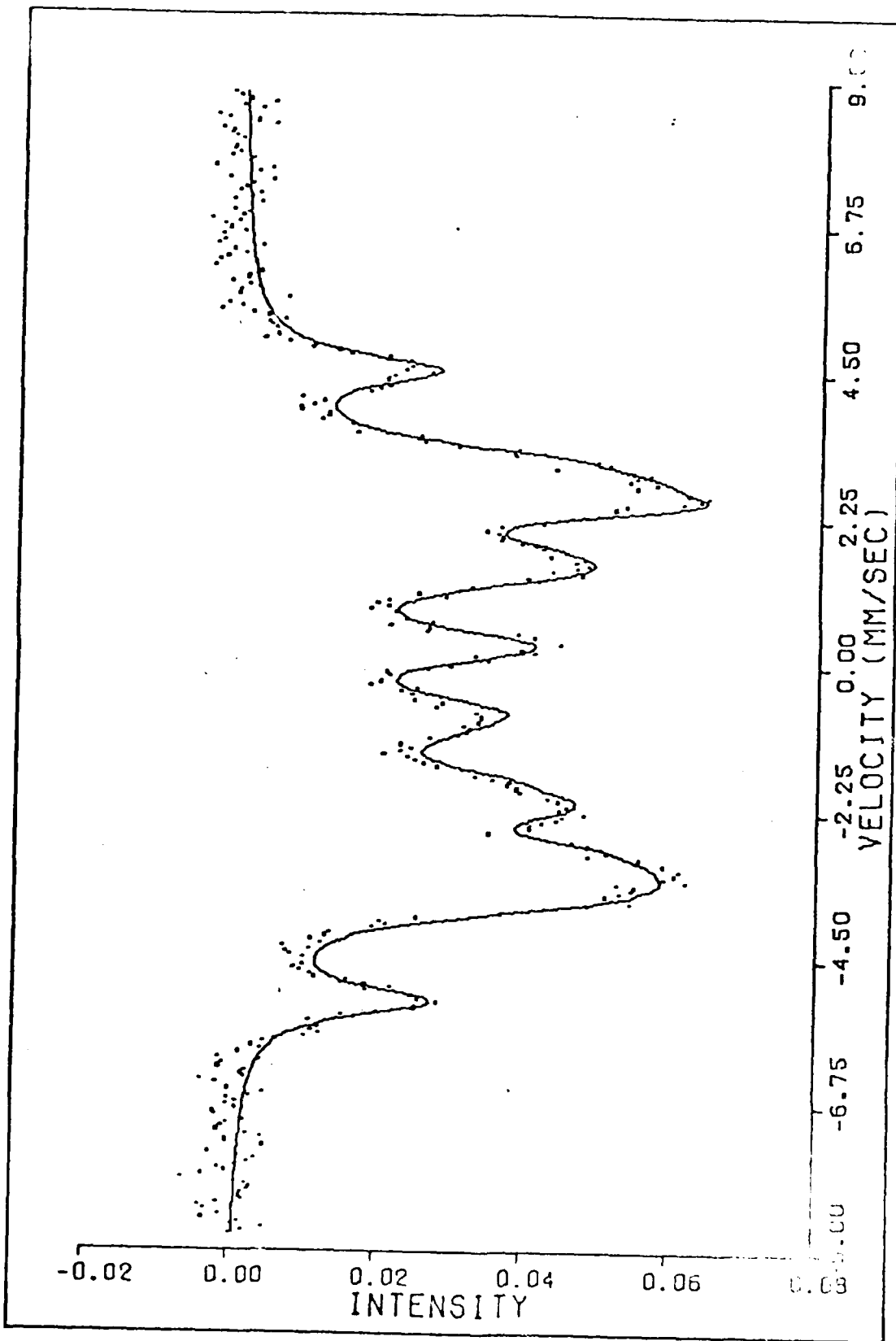


Fig. 13. Mossbauer Spectrum of  $\text{Fe}_{80}\text{B}_{20}$ , 604 K, Fully Crystallized, FIVLCALF

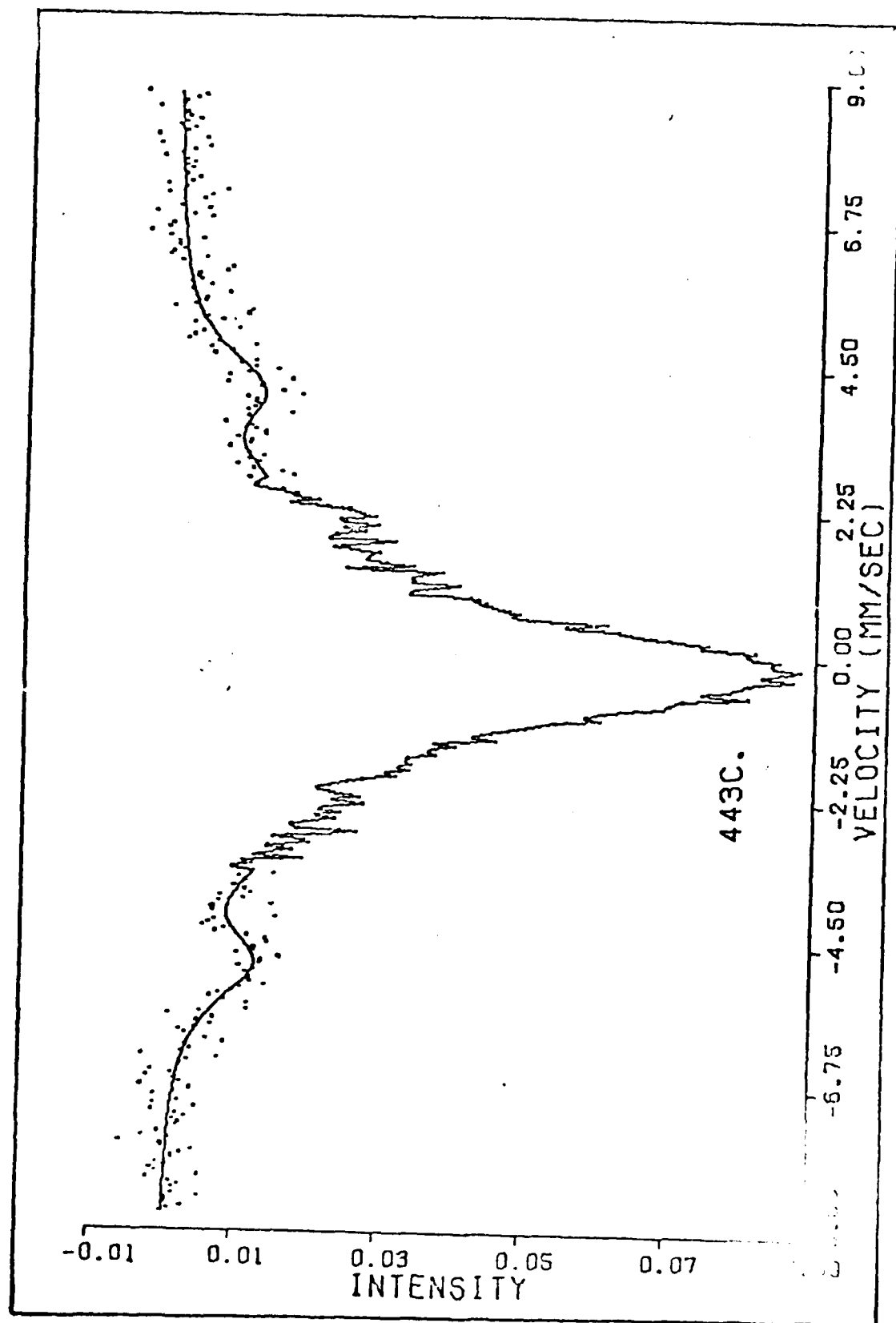


Fig. 11. Mossbauer Spectrum of  $\text{Fe}_{80}\text{P}_{6.5}\text{C}_{3.5}\text{B}_{10}$ , 716 K, 2.87 Hz, ALPHA-MG,  $x \approx 1$

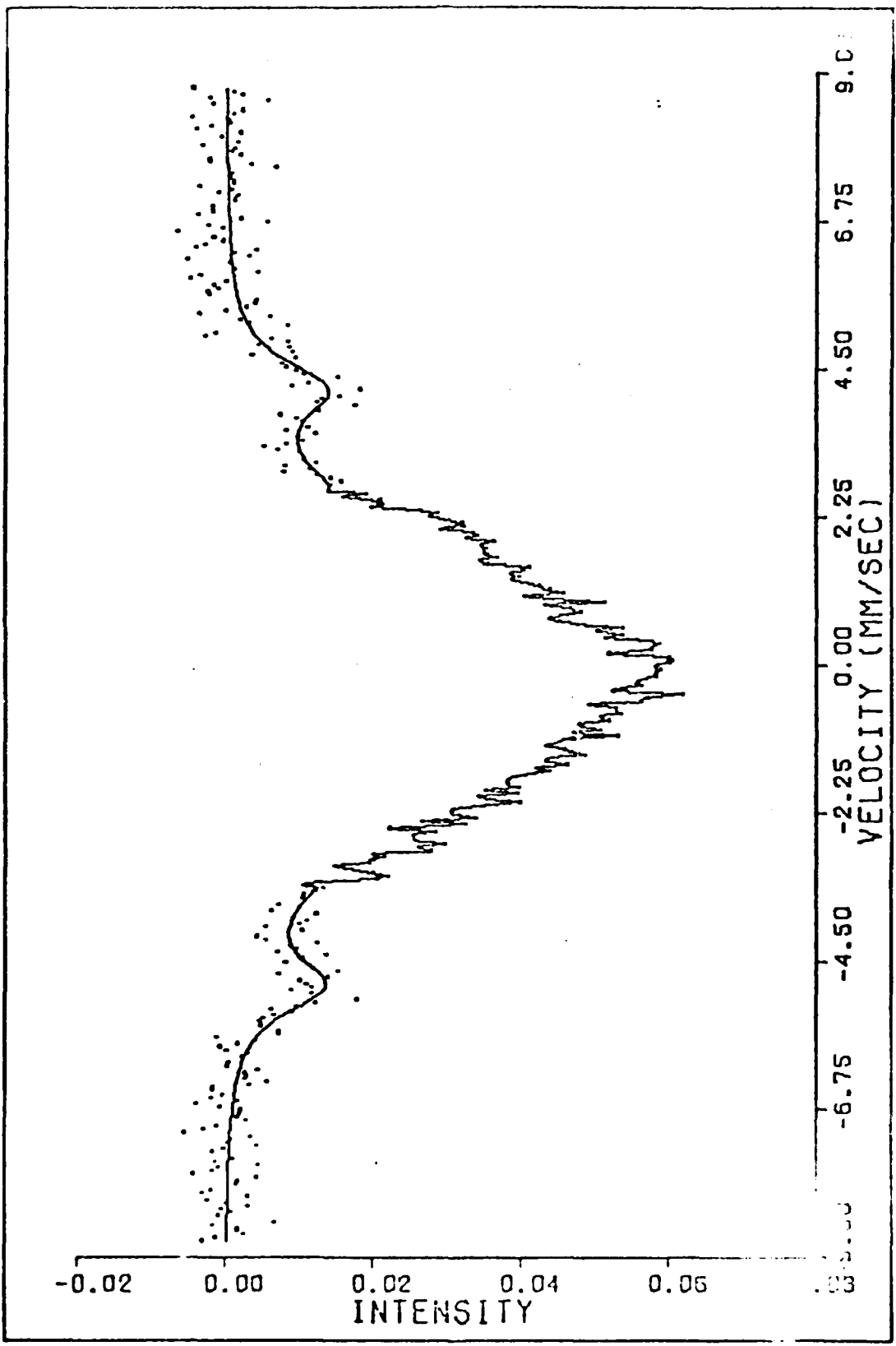


Fig. 15. Mossbauer Spectrum of  $\text{Fe}_{80}\text{P}_{6.5}\text{C}_{3.5}\text{B}_{10}$ , 716 K, Fully Crystallized  
ALPHA-BG

clearly demonstrate the effect of constraining the local quadrupole splits to zero: Chi-squared was 508 for Fig 9, but with quadrupole splitting included in FIVECALF, it was 326 (for 330 data points). Figure 11 is the fully crystallized spectrum of Run 4, and except for total intensity, it is nearly identical to Fig 9 (Run 3 at the same temperature). Figures 12 and 13 show the poorly resolved spectra obtained when using AC power for the heater. Sample motion induced by an alternating magnetic field caused extreme line-broadening which resulted in overlapping of the absorption lines. Figures 14 and 15 are two spectra obtained with  $\text{Fe}_{80}\text{P}_{6.5}\text{C}_{3.5}\text{B}_{10}$  (Run 7). Although the intensity of the  $\alpha$ -Fe peak of Fig 14 indicated a fully crystallized state, visual inspection of these two spectra show a substantial change.

The crystallized fractions for  $\text{Fe}_{80}\text{B}_{20}$  (Runs 1 thru 5) are plotted against time in Fig 16. Representative error bars are indicated on the first and last points of the 626 K data. The data of Run 4 were plotted such that the first data point fell on the calculated Run 3 line. Had the third data point been plotted on this line, the remaining points would have fallen very close to the Run 3 data. Because of low counts and line-broadening of the Mossbauer spectra of Run 2, only the last three data points were useable, and are included in Fig 16. The crystallization half lives, determined from least-squares fits to the data of Fig 16 (between  $x = 0$ , and  $x = 0.80$ ), are plotted versus time in Fig 17. The value of the activation energy  $E_A$  for  $\alpha$ -Fe crystallization was determined

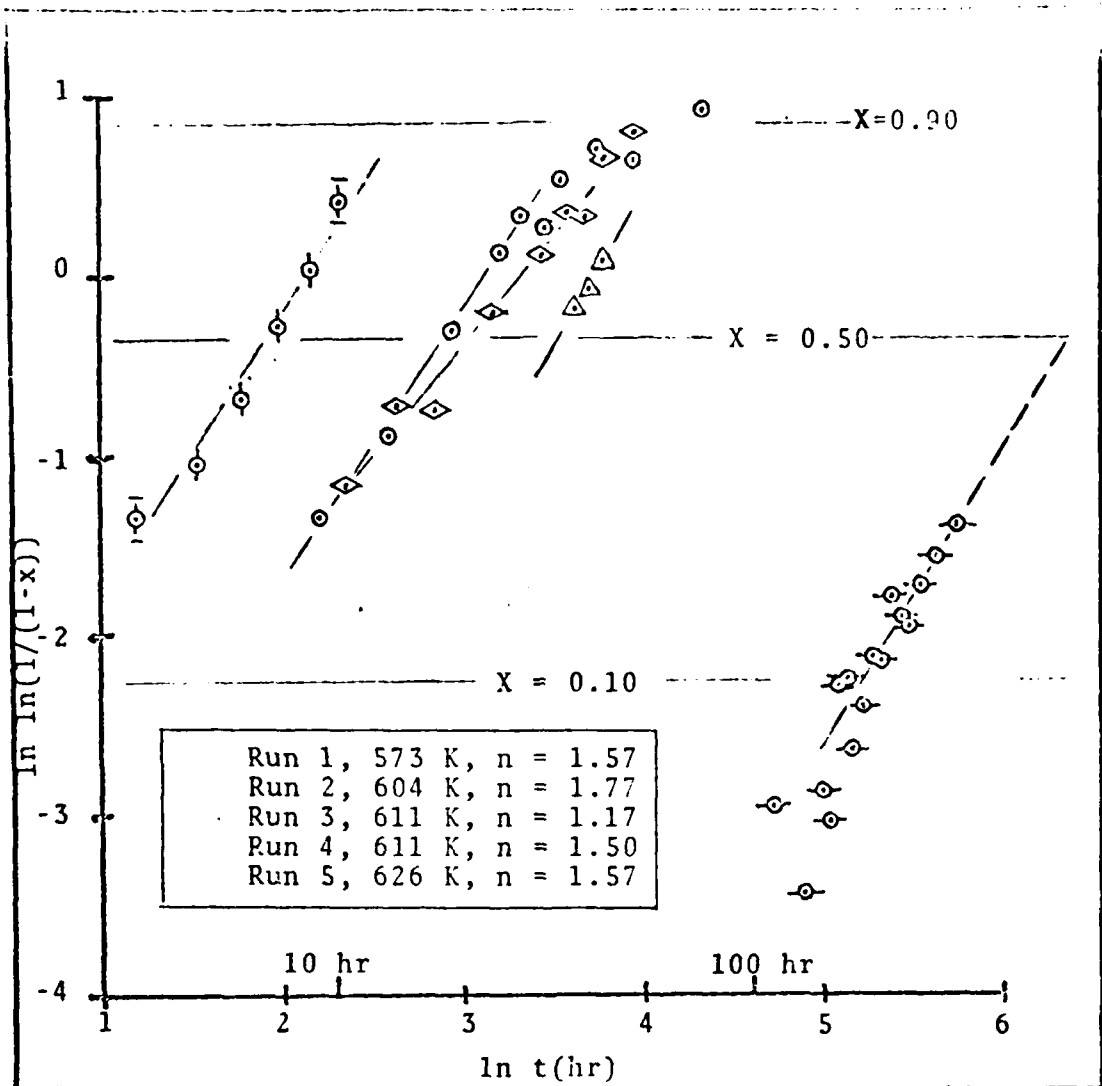


Fig 16. Crystallized Fraction  $x(t)$  vs Time,  
Plotted as  $\ln \ln(1/(1-x))$  vs  $\ln t$

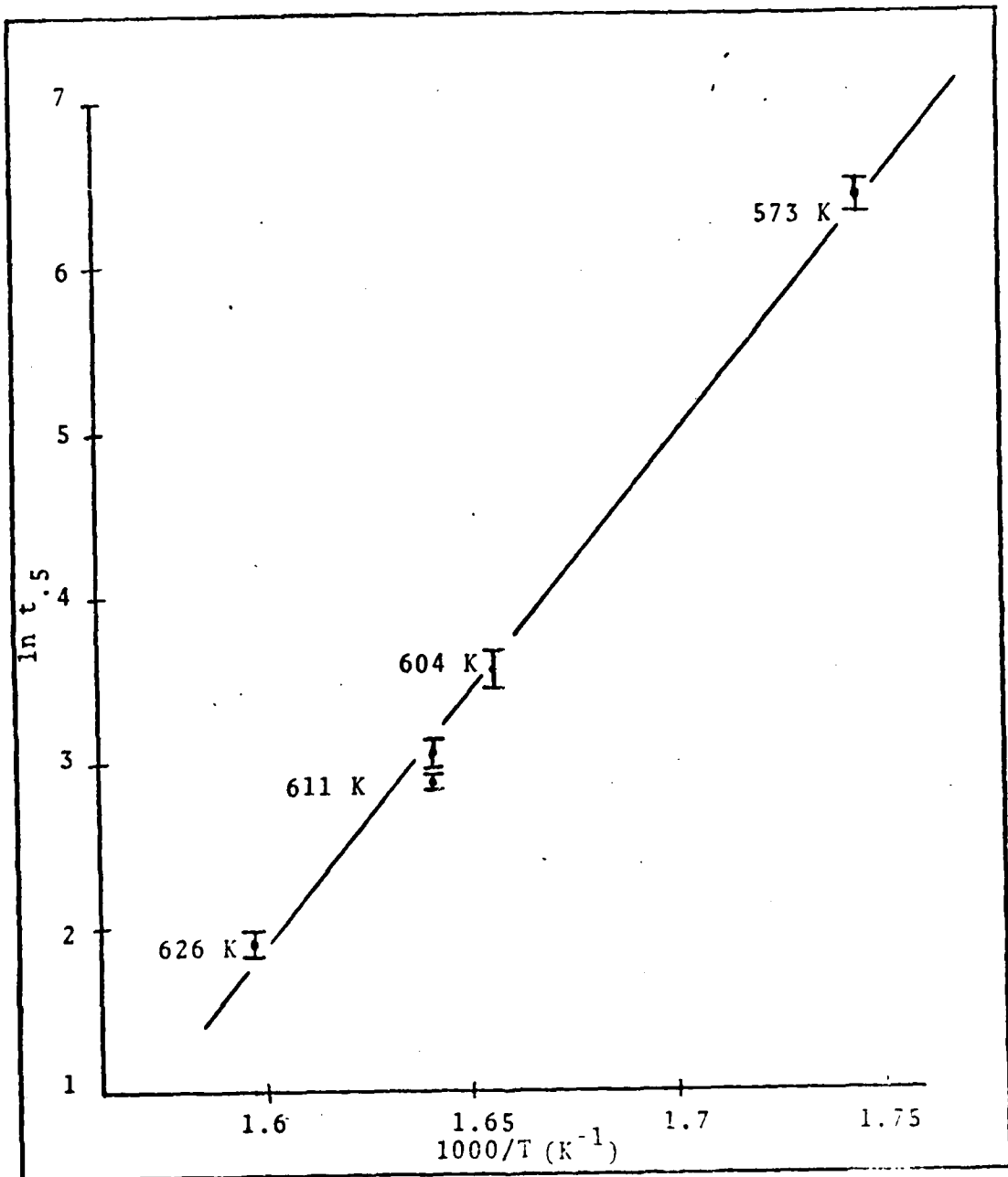


Fig 17. Arrhenius Plot. Crystallization half lives of  $\text{Fe}_{80}\text{Ni}_{20}$  versus time, plotted as  $\ln t_{0.5}$  vs  $1000/T$   
(with  $1\sigma$  error bars)

from a least-squares fit to the data of this Arrhenius plot. The value of  $E_A$  was  $0.256 \pm 0.006$  MJ/mole ( $2.65 \pm 0.007$  eV/atom), and  $\ln k_0^{-1}$  was -47.5. Using these constants and  $T = 473$  K in Eq (3), the predicted half-life of this  $\text{Fe}_{80}\text{B}_{20}$  sample is  $5500 \pm 450$  years at the expected operating temperature of 473 K.

The  $\text{Fe}_{80}\text{P}_{6.5}\text{C}_{3.5}\text{B}_{10}$  did not crystallize at 614 K, but crystallized extremely fast at 716 and 744 K. Only one or two spectra were taken before full crystallization at these two temperatures. Hence, no kinetic data were obtained for this material. Only qualitative statements can be made about the crystallization of  $\text{Fe}_{80}\text{P}_{6.5}\text{C}_{3.5}\text{B}_{10}$ ; these will be presented in the following section.

### Discussion

The values of Chi-squared obtained when analyzing the Mossbauer spectra of Runs 1 through 5 varied over a large range--from less than the number of data points for some runs to up to four times the number of data points for others. This indicates a failure of the mathematical model used to describe the Mossbauer spectra. However, this failure was expected, considering the large number of constraints on the model used for FIVECALF (the values of Chi-squared for the GAUSSCALF and ALPHA-BG fits were generally very close to the number of data points). By visual inspection, the fits were good in the area of the  $\alpha$ -Fe peaks, and its growth was probably followed accurately. The same cannot be said for the growth

of  $\text{Fe}_3\text{B}$ , due to the change in the hyperfine field and FWHM during crystallization. Since the glass spectrum does broaden slightly during crystallization, it may continue to change throughout the transformation. The fit to the  $\text{Fe}_3\text{B}$  spectra would then have to account for this change. An alternative view might be to consider the  $\text{Fe}_3\text{B}$  as still semi-amorphous during crystallization.

In Mossbauer spectra taken during early annealing runs, the values of FWHM for the  $\text{Fe}_3\text{B}$  peaks increased for peaks farther from the center. This is typical of glass spectra (Ref 16: 821). For the fully crystallized spectra, the FWHM's were nearly constant, which indicates a crystalline state. This view tends to support Kemeny's (Ref 10: 485) and Schaafsma's (Ref 11: 4429) conclusions that crystal nuclei exist in the as-quenched glass and that the structure should be based on a locally distorted, quasi-crystalline  $\text{Fe}_3\text{B}$ . It appears that the material is transformed from a glass to a semi-amorphous  $\text{Fe}_3\text{B}$ , and finally to a tetragonal  $\text{Fe}_3\text{B}$  crystal. This may be due to a stress relaxation rather than a crystallization process.

Because of the long time required to reach full crystallization at 573 K, Run 1 was terminated at 315 hrs, and the temperature was raised to 611 K. This was done to try to detect a change in the crystallization process at the lower temperature. The first crystallization time of Run 4 was adjusted by  $\Delta t$  so that this data point fell on the line calculated for Run 3. The other times of Run 4 were then adjusted by this

s , and the data was compared to that of Run 3. Because of the data scatter, no conclusion was made concerning a change in the crystallization rate or process.

Using the methods described in Chapter I, others have found the activation energy of  $\text{Fe}_{80}\text{B}_{20}$  to be between 0.195 and 0.257 MJ/mole, with the average toward the upper value (Refs 3: 42; 6: 139; 10: 485; 11: 4427). This range is significant: Luborsky, using calorimetric and magnetic methods to measure the onset of crystallization in  $\text{Fe}_{80}\text{B}_{20}$ , determined that the activation energy was 0.202 MJ/mole. He used this value to calculate an expected lifetime of 25 years at 473 K. He determined that "after the onset of crystallization, the magnetic properties deteriorate catastrophically [Ref 3: 139]."  
Schaafsma determined that the onset of crystallization corresponds to a crystallized fraction of less than 0.02 (Ref 11: 4425). Using his data, with  $E_A = 0.242$  MJ/mole, to calculate the onset of crystallization, the projected lifetime of his glass is 1000 years at 473 K. The same calculation yields a lifetime of 400 years at 473 K for the  $\text{Fe}_{80}\text{B}_{20}$  of this study. These calculations assume that the crystallization rate is determined by the growth of  $\alpha$ -Fe, not  $\text{Fe}_3\text{B}$ ; and that the crystallization mechanism does not change between 573 and 473 K.

The data obtained during the crystallization of  $\text{Fe}_{80}\text{P}_{6.5}\text{C}_{3.5}\text{B}_{10}$  were insufficient for analysis of its crystallization kinetics. However, a much higher temperature was required for crystallization. Therefore, qualitatively, its activation energy would be greater than that of  $\text{Fe}_{80}\text{B}_{20}$ . This

is true for other similar glasses with many atomic species  
(i.e.,  $\text{Fe}_{40}\text{Ni}_{40}\text{B}_{20}$ ,  $\text{Fe}_{80}\text{P}_{13}\text{C}_7$ ,  $\text{Fe}_{40}\text{Ni}_{40}\text{P}_{14}\text{B}_6$ , Ref 3: 140).  
Thus, the lifetime of  $\text{Fe}_{80}\text{P}_{6.5}\text{C}_{3.5}\text{B}_{10}$  is expected to be greater  
than that of  $\text{Fe}_{80}\text{B}_{20}$ .

## V. Conclusions and Recommendations

The metallic glasses  $Fe_{80}B_{20}$  and  $Fe_{80}P_{6.5}C_{3.5}B_{10}$  have been crystallized by isothermal annealing at high temperatures. The crystallization was followed with Mossbauer spectroscopy, and the rates of formation of  $\alpha$ -Fe crystals in  $Fe_{80}B_{20}$  were determined. These rates were used to determine the activation energy and rate constant of the crystallization process. These constants were used to calculate the expected lifetime of  $Fe_{80}B_{20}$  at 473 K, 100 K below the lowest isothermal run. If the crystallization mechanism does not change between 473 and 573 K, the onset of crystallization is projected to be approximately 400 years. No kinetic data were obtained for the crystallization of  $Fe_{80}P_{6.5}C_{3.5}B_{10}$ , or for the formation of  $Fe_3B$  in the  $Fe_{80}B_{20}$ .

### Recommendations

This study can be expanded in the following ways:

- 1) Use a stronger Mossbauer source to increase counts per channel. This would permit a more careful study of the crystallized spectra to determine  $Fe_3B$  growth rates.
- 2) Use an accurate temperature controller (with direct current), and continue the study at lower temperatures.
- 3) Study the magnetic and material properties of partially crystallized samples. This would relate crystallized fraction to material performance.

4) Since an alternating field can accelerate the aging of the glass (Ref 12), include a strong rf field during some of the isothermal annealing runs. The field strength must be great enough to displace the atoms in the amorphous metal. Kopcewicz found that 800 A/M at 67 MHz was enough to cause crystallization, but 400 A/M at 53 MHz was not.

### Bibliography

1. Schmidt, T.A. "An Analysis of Metallic Glasses by Mossbauer Spectroscopy." Unpublished MS thesis. Wright-Patterson AFB, Ohio: School of Engineering, Air Force Institute of Technology March 1978.
2. Roberts, L.D. "Mossbauer Studies of Metallic Glasses." Unpublished MS thesis. Wright-Patterson AFB, Ohio: School of Engineering, Air Force Institute of Technology, December 1978. AD A064049.
3. Luborsky, F.E. "Crystallization of Some Fe-Ni Metallic Glasses," Materials Science and Engineering, 28: 139-144 (1977).
4. Fukamichi, K., et al. "Invar-type New Ferromagnetic Amorphous Fe-B Alloys," Solid State Communications, 23(12): 955-958 (September 1977).
5. Chien, C.L. "Mossbauer Study of a Binary Amorphous Ferromagnet:  $Fe_{80}B_{20}$ ," Physical Review B, 18(3): 1003-1015 (1 August 1978).
6. Luborsky, F.E. and H.H. Lieberman. "Crystallization Kinetics of Fe-B Amorphous Alloys," Applied Physics Letters, 33(3): 233-234 (1 August 1978).
7. Tarnoczi, T., et al. "The Role of  $Fe_3B$  Compound in the Crystallization of Fe-B Metallic Glasses," IEEE Transactions on Magnetism, Mag-14(5): 1025-1027 (September 1978).
8. Matsuura, M. "Crystallization Kinetics of Amorphous Fe-B Alloys by DTA," Solid State Communications, 30(4): 231-233 (April 1979).
9. Chien, C.L., et al. "Magnetic Properties of  $Fe_xB_{100-x}$  ( $72 \leq x \leq 86$ ) and Crystalline  $Fe_3B$ ," Physical Review B, 20(1): 283-295 (1 July 1979).
10. Kemeny, T., et al. "Structure and Crystallization of  $Fe-B_x$  Metallic Glasses," Physical Review B, 20(2): 471-483 (15 July 1979).

11. Chikuma, A.S., et al. "Amorphous to Crystalline Transformation of Fe<sub>80</sub>B<sub>20</sub>," Physical Review B, 20(11): 4429-4430 (1 December 1979).
12. Kopkewicz, M. "Radio-Frequency Annealing Effects in Amorphous Fe<sub>40</sub>Ni<sub>40</sub>B<sub>20</sub>," Applied Physics, 23(1): 1-6 (September 1980).
13. May, L. An Introduction to Mossbauer Spectroscopy. New York: Plenum Press, 1971.
14. Gonser, Uli. "From a Strange Effect to Mossbauer Spectroscopy," in Topics in Applied Physics, Volume 5: Mossbauer Spectroscopy, edited by Uli Gonser. New York: Springer-Verlag, 1975.
15. Vincze, I. "Evaluation of Complex Mossbauer Spectra in Amorphous and Crystalline Ferromagnets," Solid State Communications, 25(9): 689-693 (March 1978).
16. Schurer, P.J. and A.H. Morrish. "Continuous Versus Discrete Hyperfine-Field Distributions in Amorphous Ferromagnetic Iron Alloys," Solid State Communications, 28(9): 819-823 (December 1978).
17. Hesse, J. and A. Rubartsh. "Model Independent Evaluation of Overlapped Mossbauer Spectra," Journal of Physics F, 7(6): 526-532 (June 1974).
18. Schurer, P.J. and A.H. Morrish. "Mossbauer Study of Magnetic Anisotropy in Amorphous Fe<sub>40</sub>Ni<sub>38</sub>Mo<sub>4</sub>B<sub>18</sub>," Journal of Magnetism and Magnetics, 15-18: 577-578 (1980).
19. Skluzacek, E.W. "Analysis of the Mossbauer Spectra of NdCo<sub>5</sub>." AFML-TR-75-162. Wright-Patterson AFB, Ohio: Air Force Materials Laboratory, 1976.
20. Lafleur, L.D. "Mossbauer Study of Stress-Induced Rotation of Magnetization in Amorphous Fe<sub>80</sub>B<sub>20</sub>," Physical Review B, 20(7): 2581-2585 (1 October 1979).

SUBROUTINE CALFUN(NP,NPAR,F,X)

C THIS VERSION OF CALFUN USES A GAUSSIAN LINE SHAPE TO FIT THE  
 C ABSORPTION SPECTRUM OF A METALLIC GLASS. IT GIVES ONE AVERAGE  
 C VALUE FOR HYPERFINE FIELD, ONE FOR ISOMER SHIFT, AND ONE FOR  
 C QUADRUPOLF SHIFT. IT GIVES A LINEWIDTH FOR EACH OF THE SIX  
 C PEAKS, AND THE INTENSITY RATIO OF PEAK 2 TO PEAK 1. THE AREAL  
 C RATIO FOR PEAKS 3 AND 4 TO PEAK 1 IS 1:3. THESE VALUES CAN  
 C BE SUBSTITUTED INTO THE CALFUN CALLED FIVECALF, TO PERMIT  
 C FITTING THE CRYSTALLIZED GLASS SPECTRA.

GAUSSCALF 15 OCT 80

THE REQUIRED VARIABLES ARE:

CNE VALUE FOR H-FIELD: X(1)  
 ONE VALUE OF ISOMER SHIFT: X(2)  
 ONE VALUE OF NIAD SPLIT: X(3)  
 CNE VALUE FOR TOTAL INTENSITY OF PEAK 1: X(4)  
 ONE VALUE FOR RELATIVE INTENSITY TO PEAK 1: X(5)  
 SIX VALUES OF LINE WIDTH: X(6), TO X(11)  
 BASELINE IS LAST VARIABLE: X(12)  
 TOTAL OF 12 VARIABLES REQUIRED

COMMON /HEADING/TITLE(18)

COMMON /NAME/XINIT(25),PRM(25),ERX(25),NBASE

COMMON /CALF/IFLAG

COMMON /NAME/SPIN F(LG2),X(25)

REAL V(G),MUEX,MUGND,MUSUBN,LIGHT

60 0113  
 60 0115  
 60 0120  
 60 0125  
 60 0127  
 60 0130  
 60 0133  
 60 0135  
 60 0137  
 60 0139  
 60 0140  
 60 0141  
 60 0142  
 60 0143  
 60 0144  
 60 0145  
 60 0146  
 60 0147  
 60 0148  
 60 0149  
 60 0150  
 60 0151  
 60 0152  
 60 0153  
 60 0154  
 60 0155  
 60 0156  
 60 0157  
 60 0158  
 60 0159  
 60 0160  
 60 0161  
 60 0162  
 60 0163  
 60 0164  
 60 0165  
 60 0166  
 60 0167  
 60 0168  
 60 0169  
 60 0170  
 60 0171  
 60 0172  
 60 0173  
 60 0174  
 60 0175  
 60 0176  
 60 0177  
 60 0178  
 60 0179  
 60 0180  
 60 0181  
 60 0182  
 60 0183  
 60 0184  
 60 0185  
 60 0186  
 60 0187  
 60 0188  
 60 0189  
 60 0190  
 60 0191  
 60 0192  
 60 0193  
 60 0194  
 60 0195  
 60 0196  
 60 0197  
 60 0198  
 60 0199  
 60 0200  
 60 0201  
 60 0202  
 60 0203  
 60 0204  
 60 0205  
 60 0206  
 60 0207  
 60 0208  
 60 0209  
 60 0210  
 60 0211  
 60 0212  
 60 0213  
 60 0214  
 60 0215  
 60 0216  
 60 0217  
 60 0218  
 60 0219  
 60 0220  
 60 0221  
 60 0222  
 60 0223  
 60 0224  
 60 0225  
 60 0226  
 60 0227  
 60 0228  
 60 0229  
 60 0230  
 60 0231  
 60 0232  
 60 0233  
 60 0234  
 60 0235  
 60 0236  
 60 0237  
 60 0238  
 60 0239  
 60 0240  
 60 0241  
 60 0242  
 60 0243  
 60 0244  
 60 0245  
 60 0246  
 60 0247  
 60 0248  
 60 0249  
 60 0250  
 60 0251  
 60 0252  
 60 0253  
 60 0254  
 60 0255  
 60 0256  
 60 0257  
 60 0258  
 60 0259  
 60 0260  
 60 0261  
 60 0262  
 60 0263  
 60 0264  
 60 0265  
 60 0266  
 60 0267  
 60 0268  
 60 0269  
 60 0270  
 60 0271  
 60 0272  
 60 0273  
 60 0274  
 60 0275  
 60 0276  
 60 0277  
 60 0278  
 60 0279  
 60 0280  
 60 0281  
 60 0282  
 60 0283  
 60 0284  
 60 0285  
 60 0286  
 60 0287  
 60 0288  
 60 0289  
 60 0290  
 60 0291  
 60 0292  
 60 0293  
 60 0294  
 60 0295  
 60 0296  
 60 0297  
 60 0298  
 60 0299  
 60 0300  
 60 0301  
 60 0302  
 60 0303  
 60 0304  
 60 0305  
 60 0306  
 60 0307  
 60 0308  
 60 0309  
 60 0310  
 60 0311  
 60 0312  
 60 0313  
 60 0314  
 60 0315  
 60 0316  
 60 0317  
 60 0318  
 60 0319  
 60 0320  
 60 0321  
 60 0322  
 60 0323  
 60 0324  
 60 0325  
 60 0326  
 60 0327  
 60 0328  
 60 0329  
 60 0330  
 60 0331  
 60 0332  
 60 0333  
 60 0334  
 60 0335  
 60 0336  
 60 0337  
 60 0338  
 60 0339  
 60 0340  
 60 0341  
 60 0342  
 60 0343  
 60 0344  
 60 0345  
 60 0346  
 60 0347  
 60 0348  
 60 0349  
 60 0350  
 60 0351  
 60 0352  
 60 0353  
 60 0354  
 60 0355  
 60 0356  
 60 0357  
 60 0358  
 60 0359  
 60 0360  
 60 0361  
 60 0362  
 60 0363  
 60 0364  
 60 0365  
 60 0366  
 60 0367  
 60 0368  
 60 0369  
 60 0370  
 60 0371  
 60 0372  
 60 0373  
 60 0374  
 60 0375  
 60 0376  
 60 0377  
 60 0378  
 60 0379  
 60 0380  
 60 0381  
 60 0382  
 60 0383  
 60 0384  
 60 0385  
 60 0386  
 60 0387  
 60 0388  
 60 0389  
 60 0390  
 60 0391  
 60 0392  
 60 0393  
 60 0394  
 60 0395  
 60 0396  
 60 0397  
 60 0398  
 60 0399  
 60 0400  
 60 0401  
 60 0402  
 60 0403  
 60 0404  
 60 0405  
 60 0406  
 60 0407  
 60 0408  
 60 0409  
 60 0410  
 60 0411  
 60 0412  
 60 0413  
 60 0414  
 60 0415  
 60 0416  
 60 0417  
 60 0418  
 60 0419  
 60 0420  
 60 0421  
 60 0422  
 60 0423  
 60 0424  
 60 0425  
 60 0426  
 60 0427  
 60 0428  
 60 0429  
 60 0430  
 60 0431  
 60 0432  
 60 0433  
 60 0434  
 60 0435  
 60 0436  
 60 0437  
 60 0438  
 60 0439  
 60 0440  
 60 0441  
 60 0442  
 60 0443  
 60 0444  
 60 0445  
 60 0446  
 60 0447  
 60 0448  
 60 0449  
 60 0450  
 60 0451  
 60 0452  
 60 0453  
 60 0454  
 60 0455  
 60 0456  
 60 0457  
 60 0458  
 60 0459  
 60 0460  
 60 0461  
 60 0462  
 60 0463  
 60 0464  
 60 0465  
 60 0466  
 60 0467  
 60 0468  
 60 0469  
 60 0470  
 60 0471  
 60 0472  
 60 0473  
 60 0474  
 60 0475  
 60 0476  
 60 0477  
 60 0478  
 60 0479  
 60 0480  
 60 0481  
 60 0482  
 60 0483  
 60 0484  
 60 0485  
 60 0486  
 60 0487  
 60 0488  
 60 0489  
 60 0490  
 60 0491  
 60 0492  
 60 0493  
 60 0494  
 60 0495  
 60 0496  
 60 0497  
 60 0498  
 60 0499  
 60 0500  
 60 0501  
 60 0502  
 60 0503  
 60 0504  
 60 0505  
 60 0506  
 60 0507  
 60 0508  
 60 0509  
 60 0510  
 60 0511  
 60 0512  
 60 0513  
 60 0514  
 60 0515  
 60 0516  
 60 0517  
 60 0518  
 60 0519  
 60 0520  
 60 0521  
 60 0522  
 60 0523  
 60 0524  
 60 0525  
 60 0526  
 60 0527  
 60 0528  
 60 0529  
 60 0530  
 60 0531  
 60 0532  
 60 0533  
 60 0534  
 60 0535  
 60 0536  
 60 0537  
 60 0538  
 60 0539  
 60 0540  
 60 0541  
 60 0542  
 60 0543  
 60 0544  
 60 0545  
 60 0546  
 60 0547  
 60 0548  
 60 0549  
 60 0550  
 60 0551  
 60 0552  
 60 0553  
 60 0554  
 60 0555  
 60 0556  
 60 0557  
 60 0558  
 60 0559  
 60 0560  
 60 0561  
 60 0562  
 60 0563  
 60 0564  
 60 0565  
 60 0566  
 60 0567  
 60 0568  
 60 0569  
 60 0570  
 60 0571  
 60 0572  
 60 0573  
 60 0574  
 60 0575  
 60 0576  
 60 0577  
 60 0578  
 60 0579  
 60 0580  
 60 0581  
 60 0582  
 60 0583  
 60 0584  
 60 0585  
 60 0586  
 60 0587  
 60 0588  
 60 0589  
 60 0590  
 60 0591  
 60 0592  
 60 0593  
 60 0594  
 60 0595  
 60 0596  
 60 0597  
 60 0598  
 60 0599  
 60 0600  
 60 0601  
 60 0602  
 60 0603  
 60 0604  
 60 0605  
 60 0606  
 60 0607  
 60 0608  
 60 0609  
 60 0610  
 60 0611  
 60 0612  
 60 0613  
 60 0614  
 60 0615  
 60 0616  
 60 0617  
 60 0618  
 60 0619  
 60 0620  
 60 0621  
 60 0622  
 60 0623  
 60 0624  
 60 0625  
 60 0626  
 60 0627  
 60 0628  
 60 0629  
 60 0630  
 60 0631  
 60 0632  
 60 0633  
 60 0634  
 60 0635  
 60 0636  
 60 0637  
 60 0638  
 60 0639  
 60 0640  
 60 0641  
 60 0642  
 60 0643  
 60 0644  
 60 0645  
 60 0646  
 60 0647  
 60 0648  
 60 0649  
 60 0650  
 60 0651  
 60 0652  
 60 0653  
 60 0654  
 60 0655  
 60 0656  
 60 0657  
 60 0658  
 60 0659  
 60 0660  
 60 0661  
 60 0662  
 60 0663  
 60 0664  
 60 0665  
 60 0666  
 60 0667  
 60 0668  
 60 0669  
 60 0670  
 60 0671  
 60 0672  
 60 0673  
 60 0674  
 60 0675  
 60 0676  
 60 0677  
 60 0678  
 60 0679  
 60 0680  
 60 0681  
 60 0682  
 60 0683  
 60 0684  
 60 0685  
 60 0686  
 60 0687  
 60 0688  
 60 0689  
 60 0690  
 60 0691  
 60 0692  
 60 0693  
 60 0694  
 60 0695  
 60 0696  
 60 0697  
 60 0698  
 60 0699  
 60 0700  
 60 0701  
 60 0702  
 60 0703  
 60 0704  
 60 0705  
 60 0706  
 60 0707  
 60 0708  
 60 0709  
 60 0710  
 60 0711  
 60 0712  
 60 0713  
 60 0714  
 60 0715  
 60 0716  
 60 0717  
 60 0718  
 60 0719  
 60 0720  
 60 0721  
 60 0722  
 60 0723  
 60 0724  
 60 0725  
 60 0726  
 60 0727  
 60 0728  
 60 0729  
 60 0730  
 60 0731  
 60 0732  
 60 0733  
 60 0734  
 60 0735  
 60 0736  
 60 0737  
 60 0738  
 60 0739  
 60 0740  
 60 0741  
 60 0742  
 60 0743  
 60 0744  
 60 0745  
 60 0746  
 60 0747  
 60 0748  
 60 0749  
 60 0750  
 60 0751  
 60 0752  
 60 0753  
 60 0754  
 60 0755  
 60 0756  
 60 0757  
 60 0758  
 60 0759  
 60 0760  
 60 0761  
 60 0762  
 60 0763  
 60 0764  
 60 0765  
 60 0766  
 60 0767  
 60 0768  
 60 0769  
 60 0770  
 60 0771  
 60 0772  
 60 0773  
 60 0774  
 60 0775  
 60 0776  
 60 0777  
 60 0778  
 60 0779  
 60 0780  
 60 0781  
 60 0782  
 60 0783  
 60 0784  
 60 0785  
 60 0786  
 60 0787  
 60 0788  
 60 0789  
 60 0790  
 60 0791  
 60 0792  
 60 0793  
 60 0794  
 60 0795  
 60 0796  
 60 0797  
 60 0798  
 60 0799  
 60 0800  
 60 0801  
 60 0802  
 60 0803  
 60 0804  
 60 0805  
 60 0806  
 60 0807  
 60 0808  
 60 0809  
 60 0810  
 60 0811  
 60 0812  
 60 0813  
 60 0814  
 60 0815  
 60 0816  
 60 0817  
 60 0818  
 60 0819  
 60 0820  
 60 0821  
 60 0822  
 60 0823  
 60 0824  
 60 0825  
 60 0826  
 60 0827  
 60 0828  
 60 0829  
 60 0830  
 60 0831  
 60 0832  
 60 0833  
 60 0834  
 60 0835  
 60 0836  
 60 0837  
 60 0838  
 60 0839  
 60 0840  
 60 0841  
 60 0842  
 60 0843  
 60 0844  
 60 0845  
 60 0846  
 60 0847  
 60 0848  
 60 0849  
 60 0850  
 60 0851  
 60 0852  
 60 0853  
 60 0854  
 60 0855  
 60 0856  
 60 0857  
 60 0858  
 60 0859  
 60 0860  
 60 0861  
 60 0862  
 60 0863  
 60 0864  
 60 0865  
 60 0866  
 60 0867  
 60 0868  
 60 0869  
 60 0870  
 60 0871  
 60 0872  
 60 0873  
 60 0874  
 60 0875  
 60 0876  
 60 0877  
 60 0878  
 60 0879  
 60 0880  
 60 0881  
 60 0882  
 60 0883  
 60 0884  
 60 0885  
 60 0886  
 60 0887  
 60 0888  
 60 0889  
 60 0890  
 60 0891  
 60 0892  
 60 0893  
 60 0894  
 60 0895  
 60 0896  
 60 0897  
 60 0898  
 60 0899  
 60 0900  
 60 0901  
 60 0902  
 60 0903  
 60 0904  
 60 0905  
 60 0906  
 60 0907  
 60 0908  
 60 0909  
 60 0910  
 60 0911  
 60 0912  
 60 0913  
 60 0914  
 60 0915  
 60 0916  
 60 0917  
 60 0918  
 60 0919  
 60 0920  
 60 0921  
 60 0922  
 60 0923  
 60 0924  
 60 0925  
 60 0926  
 60 0927  
 60 0928  
 60 0929  
 60 0930  
 60 0931  
 60 0932  
 60 0933  
 60 0934  
 60 0935  
 60 0936  
 60 0937  
 60 0938  
 60 0939  
 60 0940  
 60 0941  
 60 0942  
 60 0943  
 60 0944  
 60 0945  
 60 0946  
 60 0947  
 60 0948  
 60 0949  
 60 0950  
 60 0951  
 60 0952  
 60 0953  
 60 0954  
 60 0955  
 60 0956  
 60 0957  
 60 0958  
 60 0959  
 60 0960  
 60 0961  
 60 0962  
 60 0963  
 60 0964  
 60 0965  
 60 0966  
 60 0967  
 60 0968  
 60 0969  
 60 0970  
 60 0971  
 60 0972  
 60 0973  
 60 0974  
 60 0975  
 60 0976  
 60 0977  
 60 0978  
 60 0979  
 60 0980  
 60 0981  
 60 0982  
 60 0983  
 60 0984  
 60 0985  
 60 0986  
 60 0987  
 60 0988  
 60 0989  
 60 0990  
 60 0991  
 60 0992  
 60 0993  
 60 0994  
 60 0995  
 60 0996  
 60 0997  
 60 0998  
 60 0999  
 60 1000  
 60 1001  
 60 1002  
 60 1003  
 60 1004  
 60 1005  
 60 1006  
 60 1007  
 60 1008  
 60 1009  
 60 1010  
 60 1011  
 60 1012  
 60 1013  
 60 1014  
 60 1015  
 60 1016  
 60 1017  
 60 1018  
 60 1019  
 60 1020  
 60 1021  
 60 1022  
 60 1023  
 60 1024  
 60 1025  
 60 1026  
 60 1027  
 60 1028  
 60 1029  
 60 1030  
 60 1031  
 60 1032  
 60 1033  
 60 1034  
 60 1035  
 60 1036  
 60 1037  
 60 1038  
 60 1039  
 60 1040  
 60 1041  
 60 1042  
 60 1043  
 60 1044  
 60 1045  
 60 1046  
 60 1047  
 60 1048  
 60 1049  
 60 1050  
 60 1051  
 60 1052  
 60 1053  
 60 1054  
 60 1055  
 60 1056  
 60 1057  
 60 1058  
 60 1059  
 60 1060  
 60 1061  
 60 1062  
 60 1063  
 60 1064  
 60 1065  
 60 1066  
 60 1067  
 60 1068  
 60 1069  
 60 1070  
 60 1071  
 60 1072  
 60 1073  
 60 1074  
 60 1075  
 60 1076  
 60 1077  
 60 1078  
 60 1079  
 60 1080  
 60 1081  
 60 1082  
 60 1083  
 60 1084  
 60 1085  
 60 1086  
 60 1087  
 60 1088<br

```

C   LOAN VALUES OF BINOMIAL PROBABILITIES
C
C   MUEXY = .15491
MUGND = -.954206
Q=MUEXY*(MUGND*Z.)
C
C   FACTOR CONVERTS FROM ENERGY UNITS TO VELOCITY UNITS.
C
C   GZERO*MUSUBN*LIGHT*F1*F2
C   FACTOR = -----
C   2.*EZERO*F3
C
C   GZERO=.18048
MUSUBN=.6E-27
LIGHT=2.399E11
F1=.3
F2=1.0
F3=4
F7E20=14.4125E7
FR=1.6*2E-15
C
FACTR2=(GZERO*MUSUBN*LIGHT*F1*F2)/(EZERO*F3*2.)
C
A=FACTOR*(3.*R-1.)
B=FACTOR*( R-1.)
C=FACTOR*( R+1.)
C
T6((FLAG)25,25,1)
C
C   IF T6 IS NOT POSITIVE CALFUN IS BEING CAL-ED FOR PRINTING ONLY
C   AT THIS TIME
C
C   CALCULATE PEAK VELOCITIES FOR EACH SITE
C
S=X(2)
D=X(3)/2.

```

```
X(1)=ABS(X(1))
```

```
Y(1)=A*X(1)+S+Q
```

```
V(2)=D*X(1)+S-Q
```

```
V(3)=-C*X(1)+S-Q
```

```
V(4)=C*X(1)+S-Q
```

```
V(5)=-D*X(1)+S-Q
```

```
V(6)=-A*X(1)+S+Q
```

```
DO 27 I=1,11
```

```
X(I)=ANS(X(I))
```

```
33
```

```
CONTINUE
```

```
C CALCULATE THE SPECTRUM
```

```
C
```

```
25 L=X(.5)*X(7)/X(6)
```

```
TF(2*L*61*1.4) X(5)=1.4*X(6)/X(7)
```

```
DO 27 I=1,NP
```

```
X(I)=0.
```

```
I=(K-.5) K=1,E
```

```
I=(K-.5) K=1,E TI=X(L)
```

```
I=(K-.5) K=1,E TI=X(4)*X(5)
```

```
I=(K-.5) K=1,E TI=X(6)/(3.*X(8))
```

```
I=(K-.5) K=1,E TI=X(4)*X(6)/(3.*X(9))
```

```
I=(K-.5) K=1,E TI=X(4)*X(5)*X(7)/X(11)
```

```
I=(K-.5) K=1,E TI=X(4)*X(6)/X(11)
```

```
K=K+1
```

```
YYV=(X0(I)-V(K))**2/(2.*X(KP5)**.4247*X(KP5)**.4247)
```

```
TF(YYV,61*1.4) YYV=105.
```

```
YC(I)=YC(I)+(I1/SQRT(6.2832*X(KP5)**4.247**4.247))*EXP(-YYV)
```

```
YS(I)=(1.-YC(I))*X(NBASE)
```

```
FC(I)=(YD(I)-YC(I))/SQRT(YD(I))
```

```
RETURN
```

```
35
```

```
ON THE FINAL CALL OF CALFUN PRINT THE PEAK VELOCITIES
```

```
C
```

```
CONTINUE
```

```
25
```

```
PRINT 90
```

```
DO 1173
```

```
60 1173
```

```
61 1173
```

```
62 1173
```

```
63 1173
```

```
64 1173
```

```
65 1173
```

```
66 1173
```

```
67 1173
```

```
68 1173
```

```
69 1173
```

```
70 1173
```

```
60 1173
```

```
61 1173
```

```
62 1173
```

```
63 1173
```

```
64 1173
```

```
65 1173
```

```
66 1173
```

```
67 1173
```

```
68 1173
```

```
69 1173
```

```
70 1173
```

```
71 1173
```

```
72 1173
```

```
73 1173
```

```
74 1173
```

```
75 1173
```

```
76 1173
```

```
77 1173
```

```
78 1173
```

```
79 1173
```

```
80 1173
```

```
81 1173
```

```
82 1173
```

```
83 1173
```

```
84 1173
```

```
85 1173
```

```
86 1173
```

```
87 1173
```

```
88 1173
```

```
89 1173
```

```
90 1173
```

```
91 1173
```

```
92 1173
```

```
93 1173
```

```
94 1173
```

```
95 1173
```

```
96 1173
```

```
97 1173
```

```
98 1173
```

```
99 1173
```

```
POINT *, " "
POINT *, " "
POINT *, " THE PEAK VELOCITIES ARE: "
POINT *, " "
POINT 100, (V(I), I=1,6)
POINT *, " "
POINT *, " "
POINT *, " "
FORMAT (1H1)
FORMAT (5X,7F16.4)
SETIF N
END
```

```
9C1210
9C1250
6B1250
6C1270
6C1270
6C1290
6C1290
6C1290
6C1290
6B1310
6B1310
6C1310
6C1320
6C1320
6B1340
```

SUBROUTINE CALFUN(NP,NPAR,F,X)

```

C CALFUN USES SUPERPOSITION OF FIVE 5-SPEAK SPECTRA: ONE FOR
C ALPHA-FE, THREE FOR FE38, AND ONE FOR THE GLASS. THE VARIABLE
C PARAMETERS ARE LISTED BELOW. THE LINWIDTH FOR ALPHA-FE MUST
C BE ANDED AT LINE 173!. AREA RATIOS ARE NORMALIZED TO PEAK 1
C FOR EACH SPECTRUM. ALL THREE FE38 SPECTRA ARE REQUIRED TO HAVE
C THE SAME AMPLITUDE, AND AREA RATIOS FOR PEAKS 1:2:3:4:5:6 OF
C 3:2:1:1:2:3. FOR THE GLASS SPECTRUM, ONLY THE INTENSITY IS A
C VARIABLE PARAMETER, THE OTHERS MUST BE SUPPLIED IN LINES 146!
C TO 143! AND 182! TO 192!. THIS CALFUN ALSO GIVES THE COUNTS
C ASSORBED BY ALPHA-FE AND THE TOTAL COUNTS ABSORBED. THIS VERSION
C OF FIVECALF IS FOR 336 C DATA ONLY.

```

FIVECALF 22 NOV 80

THE REQUIRED VARIABLES ARE:

```

C ONE VALUE OF H-FIELD FOR ALPHA IRON: X(1)
C THREE VALUES OF H-FIELD FOR FE38: X(2) TO X(4)
C ONE VALUE OF TOTAL INTENSITY FOR ALPHA FE: X(5)
C ONE VALUE OF TOTAL INTENSITY FOR FE38: X(6) TO X(9)
C THREE VALUES OF LINewidth FOR FE38: X(7) TO X(9)
C ONE VALUE OF ISOMER SHIFT FOR ALPHA FE: X(10)
C THREE VALUES OF ISOMER SHIFT FOR FE38: X(11) TO X(13)
C ONE VALUE OF TOTAL INTENSITY FOR THE FE38: X(14)
C ONE VALUE OF TOTAL INTENSITY FOR THE FE38: X(15)
C BASELINE IS LAST VARIABLE: X(15)
C TOTAL OF 15 VARIABLES REQUIRED

```

```

C      COMMON W(13(2)),X0(402),Y0(402),YDY(402),YCY(402),FSN(402) U 2170
C      COMMON /HEADINGS/TITL(18)          U 2150
C      COMMON /NAME/XINIT(25),PRN(25),ERX(25),NRASE U 2150
C      COMMON /CALF/IFLAG U 2150
C      DIMENSION F(4(2)),X(25)          U 2150
C      REAL V(30),MUEX,MUSUBN,LIS4f,H,B1(5) U 2150
C
C
C      MUEX=.1!+91
C      MUEND=-.1!+21E
C      R=MUE X/(MUEND*3.)
C
C      FACTOR CONVERTS FROM ENERGY UNITS TO VELOCITY UNITS.
C
C
C      GZERO=MUSUBN*LIGHT*F1*F2
C      FACTOR = -----
C      2.*EZERO*F3
C
C      GZERO=1.0000
C      MUSUBN=5.05E-27
C      LIGHT=2.99E11
C      F1=1.0E3
C      F2=1.0E-4
C      EZERO=16.4125E3
C      F3=1.5E-19
C
C      FACTOR=(GZERO*MUSUBN*LIGHT*F1*F2)/(EZERO*F3*2.)
C
C      FACTOR = -----
C      R = FACTOR ( R-1. )
C      R = FACTOR ( R+1. )
C
C      IF(IFLAG)25,25,17
C
C      IF IFLAG IS NOT POSITIVE CALFUN IS BEING CALLED FOR PRINTING ONLY

```

```

C      CONTINUE
C      CALCULATE PEAK VELOCITIES FOR EACH SITE
C
C      NO 11 I=1,9
11    X(1)=ABS(X(1))
C
C      THE FOLLOWING IS FOR THE ALPHA IRON SPECTRUM.
C      H IS THE HYPERFINE FIELD AND S IS THE ISOMER SHIFT.
C      V(1) TO V(6) ARE THE VELOCITIES OF PEAKS ONE TO SIX.
C
H=X(1)
S=X(11)
V(1)=A*H+S
V(2)=L*H+S
V(3)=-C*H+S
V(4)=C*H+S
V(5)=-D*H+S
V(6)=-A*H+S
C
C      THE FOLLOWING IS FOR THE FIRST FE33 SPECTRUM.
C
H=V(2)
S=X(11)
I=1.
V(7)=A*H+S+0
V(15)=D*H+S-0
V(19)=-C*H+S-0
V(23)=C*H+S-0
V(14)=-D*H+S-0
V(8)=-A*H+S+0
C
C      THE FOLLOWING IS FOR THE SECOND FE33 SPECTRUM.
C
H=X(3)

```





```

      YC(I)=(T/I)/SORT(1.133+31*(K-24)*2)+EXP(-YYY)
C   CALCULATE COUNTS ABSORBED BY ALPHA-AFE.
C
      33    TF(K,LT,J)  AAFE=AAFE+YCP
      35    YC(I)=YC(I)+YCP
C
      36    CALCULATE TOTAL COUNTS ABSORBED.
C
      36    ATOT=ATOT+YC(I)
      YC(I)=(1.-YC(I))*X(NBASE)
      F(I)=(YD(I)-YC(I))/SORT(YD(I))
      R=F(J)?N
C
      37    ON THE FINAL CALL OF CALFUN PRINT THE PEAK VELOCITIES AND
      37    THE COUNTS ABSORBED.
C
      25    COUNT NUE
      POINT 92
      FORMAT(1H1,/,38H THE PEAK VELOCITIES ARE (IN KM/SEC):,,/)
      PRINT 1:,,(V(I)),I=1,6)
      POINT 93
      FORMAT(//,F3H THE PEAK VELOCITIES FOR THE THREE FE33 SPECTRA ARE:
      1,/,)
      DO 35 I=7,11,2
      POINT 1:,,(V(I),V(I+5),V(I+12),V(I+13),V(I+7),V(I+1))
      POINT 94
      POINT 91,AAFE
      FORMAT(1H1,/,L3H THE TOTAL ALPHA IRON AREA (SIX PEAKS) IS://,
      1F4.0,/,/,/,)
      POINT 95,ATOT
      POINT 95,37H THE AREA UNDER THE ENTIRE CURVE IS:,,/,,F10.4)
      POINT 96
      POINT 96
      POINT 97,ATOT(1H1)
      POINT 97,37H
      POINT 98,FONCAT(5X,7F10.4)
      RETURN
      END

```

## SUBROUTINE CALFUN(NP,NPAR,F,XI)

C THIS CALFUN FILLS ONLY PEAKS ONE AND SIX OF THE ALPHA-FE SPECTRUM.  
C IT ADDS A GAUSSIAN SHAPED BACKGROUND TO THE ALPHA-FE TO ACCOUNT FOR  
C THE CLOSNESS OF THE GLASS SPECTRUM TO THE CRYSTALLIZED ALPHA-FE  
C SPECTRUM. IT FITS THE CENTER PORTION OF THE SPECTRUM WITH THE  
C APPROXIMATE DATA VALUES.

ALPHA-BG 22 OCT 89

THE REQUIRED VARIABLES ARE:

ONE VALUE OF H-FIELD FOR ALPHA IRON: X(1)

ONE VALUE OF H-FIELD FOR THE BACKGROUND CURVE: X(2)

ONE VALUE OF ISOMER SHIFT FOR ALPHA IRON: X(3)

ONE VALUE OF ISOMER SHIFT FOR THE BACKGROUND CURVE: X(4)

TWO VALUES OF LINE WIDTH: X(5) TO X(6)

ONE VALUE OF TOTAL INTENSITY OF PEAK 1: X(7)  
FOR ALPHA IRONONE VALUE OF TOTAL INTENSITY OF THE BACKGROUND: X(8)  
BASELINE IS LAST VARIABLE: X(9)

TOTAL OF 9 VARIABLES REQUIRED

COMMON W(13), XC, XD(4,2), YD(4,2), Y2(4,2), YDY(4,2), YCY(4,2), FS3(4,2)  
COMMON /HEADING/TITL(18)  
COMMON /NAME/XINIT(25), PRM(25), ERX(25), NRASE

## APPENDIX C

## ALPHA-BG

```
CONVON /CALF/ IFLAG  
DIMENSION F(12),X(25)  
REAL V(6),MUEX,MUGND,MUSUBN,LIGHT
```

### LOAN VALUES OF BINOMIAL PROBABILITIES

```
MUEX=.15E91  
MUSUBN=-.19E25E  
R=4JEX/(MUGND*3.)
```

```
FACTOR CONVERTS FROM ENERGY UNITS TO VELOCITY UNITS.
```

```
GZERO*MUSUBN*LIGHT*F1*F2  
FACTOR = -----  
2.*ZERO*F3
```

```
G7E20=.16E48  
MUSUBN=.15E-27  
LIGHT=2.*99E11  
F1=1.*.9E3  
F2=1.*.8E-4  
ZERO=.14.*4125E3  
FR=1.*.6E2E-15
```

```
FACTOR=(G7E0*MUSUBN*LIGHT*F1*F2)/(ZERO*F3*2.)
```

```
A=FACTOR*(3.*R-1.)  
D=FACTOR*( R-1.)  
C=FACTOR*( F+1.)
```

```
IF(IFLAG)25,25,15
```

```
1 IF IFLAG IS NOT POSITIVE CALFUN IS BEING CALLED FOR PRINTING ONLY
```

```
2 CONTINUE
```

```
3 C  
4 C
```

```
C31550  
C315450  
C315420  
C315380  
C315350  
C315320  
C315290  
C315260  
C315230  
C315200  
C315170  
C315140  
C31510  
C315070  
C315040  
C315010  
C315000  
C314970  
C314940  
C314910  
C314880  
C314850  
C314820  
C314790  
C314760  
C314730  
C314700  
C314670  
C314640  
C314610  
C314580  
C314550  
C314520  
C314500  
C314470  
C314440  
C314410  
C314380  
C314350  
C314320  
C314290  
C314260  
C314230  
C314200  
C314170  
C314140  
C314110  
C314080  
C314050  
C314020  
C314000
```

```

C CALCULATE PEAK VELOCITIES FOR EACH SITE
C
      DO 14 I=1,2
11      X(I)=ARS(X(1))
      V(1)=A*X(1)+X(3)
      V(2)=A*X(2)+X(4)
      V(3)=-A*X(2)+X(4)
      V(4)=-A*X(1)+X(3)
      DO 13 I=5,5
13      X(I)=ARS(X(I))
      20 NTT NUE
C
C CALCULATE THE SPECTRUM
C
      AAFF=0.0
      ATOT=0.0
      DO 3 Y=1,NP
      IF(I.LT.102 .OR. I.GT.214) GO TO 31
      YC(I)=1-(0.45*YD(I-1)+0.35*YD(I+1)+0.39*YD(I))/X(NBASE)
      GO TO 36
      YC(I)=0.
31      DO 35 K=1,4
      IF(K.EQ.1 .OR. K.EQ.4) TI=X(7)
      IF(K.EQ.2 .OR. K.EQ.3) TI=X(8)
      IF(K.EQ.2 .OR. K.EQ.3) GO TO 32
      YC=TI*((XD(I)-V(K))*2*4.)/X(5)**2+1.0
      AAFF=AAFE+YCP
      GO TO 35
      YYY=(XD(1)-V(K))**2/(2.+(0.42+.7*X(5))**2)
      IF(YYY.GT.1.0) YYY=1.0.
      YD=TT/SQRT((0.2836)/.4247/X(6)*EXP(-YYY))
      YC(I)=YC(I)+YCF
      ATOT=ATOT+YC(I)
      YC(I)=(1.-YC(I))*X(NBASE)
      F(I)=(YD(I)-YC(I))/SORT(YD(I))
      RETURN
32      ON THE FINAL CALL OF CALFUN PRINT THE PEAK VELOCITIES
C
      CONTINUE
25

```

```

PRINT 9F
PRINT ",," "
PRINT ",," "
PRINT ",," THE PEAK VELOCITIES AREA"
PRINT ",," "
PRINT 10L,(V(I),I=1,4)
PRINT ",," "
PRINT ",," "
PRINT ",," "THE AREA UNDER PEAKS 1 AND 5 OF ALPHA IRON IS: ",A=FE
PRINT ",," THE TOTAL ALPHA IRON AREA IS TWICE THAT AREA."
PRINT ",," "
PRINT ",," "
PRINT ",," "THE AREA UNDER THE ENTIRE CURVE IS: ",ATOT
PRINT ",," "
PRINT ",," "
PRINT 9C
FORMAT(1H1)
FORMAT(5X,7F1E+4)
RETURN
END

```

30  
105

## APPENDIX D

### GENFIT Instructions

This appendix contains instructions for using GENFIT with one of the three CALFUNs listed in Appendices A, B, and C. It is presented in two parts; the first explains the control cards and parameters used when running GENFIT, the second describes how to alter FIVECALF for different temperature runs.

#### Control Deck

The following control deck precedes the data. It permits processing on the AFIT terminal only.

```
DEB,T300,CM120000,STCSB. M799999,DBELLER,4369.  
ATTACH,A,GENFIT,MR=1  
FIN,I=A,OPT=0,R=2,L=0.  
ATTACH,COMPILE,GAUSSCALF,MR=1  
FIN,I,OPT=0,R=2,L=0.  
ATTACH,P,CCPLOT56X,ID=LIBRARY,SN=ASD.  
LIBRARY,P.  
LDSET,PRESET=ZERO  
LGO.  
7/8/9
```

The first two cards of the data deck are title cards. They are used to identify the material and run number, and the CALFUN used for processing the data. The third data card contains processing parameters as explained below.

FEB1(11/13)80. 611 X.  
FIVCALI

12,188,218,2,1,200,0.

includes baseline as a variable parameter

maximum calls of CALFUN

type of plot

number of times timing channels have  
exceeded one million counts

}GENFIT does not fit the velocity curve

}between these channel numbers

number of variable parameters in the  
attached CALFUN

The parameter cards then follow this card. In this case, there are twelve (as in above card). TWC are given for example (format I6, open):

HFIELD 310.

.

.

.

.

BASELN 52000

The Mossbauer data deck follows immediately after the parameter cards. There are forty data cards, in I3, 10I7 format. They contain the channel number of the first data entry on each card plus 10 channels of data. The final two cards contain more processing parameters.

1, 1, 2, 21, 60, 550, 505, 0

- number of times the data is smoothed before processing
- range of channels of right-hand zone for polynomial baseline fitting
- range of channels of left-hand zone for polynomial baseline fitting
- number of zones to be used for baseline fitting
- number of times baseline has exceeded one million counts
- order of the polynomial fit to the baseline

9.0, 2.25

- distance between tick marks on the horizontal (velocity) scale of the CALCOMP plot, in mm/sec
- horizontal scale distance (-9 to +9 mm/sec)

The final card for processing Mossbauer data is the end-of-job card:

6/7/8/9 END OF JOB

#### Altering FIVECALF

FIVECALF must be changed for different temperature runs because the glass spectrum changes over a given temperature range. The average hyperfine field, the distribution of fields, the relative intensity of peak two to peak one, and the isomer shift and quadrupole split all vary with temperature. Altering FIVECALF is rather simple, however. Once GAUSSCALF has been run with a non-crystallized spectrum and the parameters

obtained, the necessary changes to FIVECALF can be made.

They are listed below by line number in Appendix B.

- 000220 change temperature to that which this copy of FIVECALF will be for
- 001460 change H=145. to the hyperfine field obtained with GAUSSCALF
- 001470 change S=-.200 to the isomer shift obtained
- 001480 change Q=-.005 to the quadrupole split obtained
- 001840 change B1(1) to the value obtained for the linewidth of peak one
- 001850 change B1(2) to the value obtained for the linewidth of peak two
- 001860 change B1(3) to the value obtained for the linewidth of peak three
- 001870 change B1(4) to the value obtained for the linewidth of peak four
- 001880 change B1(5) to the value obtained for the linewidth of peak five
- 001890 change B1(6) to the value obtained for the linewidth of peak six
- 001950 change 1.30 to the value of the ratio of peak two to peak one
- 001980 change 1.30 to the value of the ratio of peak two to peak one

## APPENDIX E

### Applications of Metallic Glasses

In this appendix some of the existing and proposed applications of the metallic glasses are described. The mechanical, electrical, and magnetic properties of some of the glasses make them suitable for many uses. Two commercial applications have existed since 1976. A woven fabric has been manufactured for use as magnetic shielding. It performs as well as  $Fe_{80}Ni_{20}$  foil, and it has the advantage of high flexibility. The other current application of metallic glass is in magnetostriuctive delay lines, which take advantage of the large magnetostriction of the metallic glasses and the high change in Young's modulus with applied magnetic field. Other uses are envisioned which take advantage of various combinations of magnetic "softness," mechanical hardness, and high electrical resistivity.

Due to the ease of reversing magnetic fields in the metallic glasses, power transformers with these materials in their cores would lose much less energy to heating. These glassy metals have been proposed for winding the cores of inversion transformers, current and pulse transformers, and magnetic amplifiers. They also are likely candidates for the "read" and "write" heads in magnetic tape recorders and disc

new systems. Their electrical resistance properties make them suitable for electrical resistors, low temperature heating wires, and resistance thermometers.

The various mechanical properties of the glassy metals make them useful for many other applications. Because of high tensile strength, some of the glasses might be used as reinforcing filaments in tires, transmission belts, or high pressure tubing; or as stress transducers in a multi-vibrator configuration. Their corrosion resistance makes them useful in underwater cables or biomaterials. The hardness and ability to be sharpened make some of the glassy metals suitable materials for manufacturing cutting devices.

Besides the above applications which are based on the macro-properties of the metallic glasses, there is at least one use based on their micro-structure: they have been proposed as the storage medium for magnetic "bubble" memory systems. Since the bubbles in the metallic glasses are one-fifth the size of those in synthetic garnet, the storage density would be 25 times greater. The vortices (important in superconductors) are 10 times smaller. If these can be used for storage, the information density could be 250 times greater than that now projected in synthetic garnet bubble memory systems.

All of the above applications can take advantage of two common properties of the metallic glasses: they are very easy to work with, due to their flexible-fiber form; and they are inexpensive to manufacture, due to the one-step production

process, with no subsequent treatments necessary. A few of the authors who have researched the applications of the metallic glasses--and will probably continue--are: C.D. Graham, T. Egami, J.J. Gilman, P. Chaudhari, and F.E. Luborsky.

Vita

Denis Eugene Beller was born on November 22, 1950, in Okmulgee, Oklahoma, and is the son of Ernest E. and Ezma I. Beller. He graduated from Norte Del Rio High School in Sacramento, California in June 1968. He attended the University of Nevada and American River College before enlisting in the Air Force in 1971. In May 1976 he graduated with honors from the University of Colorado with a degree of Bachelor of Science in Chemical Engineering. Following graduation from Air Force Officer Training School, he served as a test engineer at the Air Force Rocket Propulsion Laboratory, Edwards AFB, California. Prior to attending the Air Force Institute of Technology, he served as a test section chief and senior test engineer at Edwards. He and his wife Judy have two sons.

Permanent Address: 2101 Middleberry Rd.  
Sacramento, Ca. 95815

## UNCLASSIFIED

SECURITY CLASSIFICATION OF THIS PAGE (When Data Entered)

REPORT DOCUMENTATION PAGE		READ INSTRUCTIONS BEFORE COMPLETING FORM
1 REPORT NUMBER AFIT/GNE/PH/81M-1	2 GOVT ACCESSION NO. AD-A100 818	3 RECIPIENT'S CATALOG NUMBER
4 TITLE (and Subtitle) CRYSTALLIZATION KINETICS OF TWO METALLIC GLASSES BY MOSSBAUER SPECTROSCOPY	5 TYPE OF REPORT & PERIOD COVERED MS Thesis	
7 AUTHOR(S) Denis L. Beller Captain, USAF	6 PERFORMING ORG. REPORT NUMBER	
9 PERFORMING ORGANIZATION NAME AND ADDRESS Air Force Institute of Technology (AFIT/EN) Wright-Patterson AFB, Ohio 45433	10 PROGRAM ELEMENT, PROJECT, TASK AREA & WORK UNIT NUMBERS	
11 CONTROLLING OFFICE NAME AND ADDRESS	12 REPORT DATE 7 March 1981	
14 MONITORING AGENCY NAME & ADDRESS (if different from Controlling Office)	13 NUMBER OF PAGES 75	
	15 SECURITY CLASS. (of this report) UNCLASSIFIED	
	15a. DECLASSIFICATION/DOWNGRADING SCHEDULE	
16 DISTRIBUTION STATEMENT (of this Report) Approved for public release; distribution unlimited.		
17 DISTRIBUTION STATEMENT (of the abstract entered in Block 20, if different from Report)		
APPROVED FOR PUBLIC RELEASE AFR 17 1861 NOV 11		
18 SUPPLEMENTARY NOTES <b>APPROVED</b> ASE AFR 190-12	<i>Audrie C. Lynch</i> FREDRIC C. LYNN, Major USAF Director of Public Affairs	
19 KEY WORDS (Continue on reverse side if necessary and identify by block number) Metallic Glasses Aging Kinetics Fe <sub>80</sub> B <sub>20</sub>	Crystallization Kinetics Mossbauer Spectroscopy Air Force Institute of Technology (AFIT) Wright-Patterson AFB, OH 45433	
20 ABSTRACT (Continue on reverse side if necessary and identify by block number) In this study, Mossbauer spectroscopy was used to examine thermal aging of two metallic glasses. Fe <sub>80</sub> B <sub>20</sub> was isothermally annealed at 573, 604, 611, and 626 K, and Fe <sub>80</sub> P <sub>6.5</sub> C <sub>3.5</sub> B <sub>10</sub> was annealed at 614, 716, and 744 K. The activation energy of Fe <sub>80</sub> B <sub>20</sub> , determined from the growth of		

UNCLASSIFIED

SECURITY CLASSIFICATION OF THIS PAGE(When Data Entered)

Block 20:

+ or -

$\alpha$ -Fe crystals, was  $0.256 \pm 0.006$  MJ/mole. The projected lifetime of this glass, based on the onset of crystallization, is 400 years. No quantitative data were obtained for Fe<sub>80</sub>P<sub>6.5</sub>C<sub>3.5</sub>B<sub>10</sub>; however, based on the higher temperature required for crystallization, it is expected to have a longer lifetime.

UNCLASSIFIED

SECURITY CLASSIFICATION OF THIS PAGE(When Data Entered)

END

DATE

FILMED

7 - 81

DTIC